A new terrestrial analogue site for Mars research: the Qaidam Basin, Tibetan Plateau (NW China)

Long Xiao, Jiang Wang, Yanan Dang, Ziye Cheng, Ting Huang, Jiannan Zhao, Yi Xu, Jun Huang, Zhiyong Xiao, Goro Komatsu

PII: S0012-8252(16)30174-X
DOI: doi:10.1016/j.earscirev.2016.11.003
Reference: EARTH 2344

To appear in: *Earth Science Reviews*

Received date: 20 July 2016
Revised date: 7 November 2016
Accepted date: 10 November 2016

Please cite this article as: Xiao, Long, Wang, Jiang, Dang, Yanan, Cheng, Ziye, Huang, Ting, Zhao, Jiannan, Xu, Yi, Huang, Jun, Xiao, Zhiyong, Komatsu, Goro, A new terrestrial analogue site for Mars research: the Qaidam Basin, Tibetan Plateau (NW China), *Earth Science Reviews* (2016), doi:10.1016/j.earscirev.2016.11.003

A new terrestrial analogue site for Mars research: the Qaidam Basin, Tibetan Plateau (NW China)

Long Xiao [1, 2], Jiang Wang [1], Yanan Dang [2], Ziye Cheng [1], Ting Huang [1], Jiannan Zhao [1], Yi Xu [2], Jun Huang [1], Zhiyong Xiao [1], Goro Komatsu[3]

1. State Key Laboratory of Geological Process and Mineral Resources, Planetary Science Institute, School of Earth Sciences, China University of Geosciences, Wuhan, 430074 China

2. Space Science Institute, Lunar and Planetary Science Laboratory, Macau University of Science and Technology, Taipa, Macau, China

3. International Research School of Planetary Sciences, Università d'Annunzio, Viale Pindaro 42, 65127 Pescara, Italy

Abstract

Remote sensing observations and rover missions have documented the presence of playas, salts, and wind erosion landforms of lacustrine sediments on Mars. All of these observations suggest Mars was aqueous in its early history. However, abundant questions remain: How wet was the environment, what were the properties of the liquids and the possibility of ancient habitability,, and what kinds of geological processes shaped the present landforms? To explore these unknowns, analogue studies can play a key role. In this contribution, we introduce the Qaidam Basin, Tibetan Plateau, northwestern China as a new and unique analogue site for studying the past aqueous and present arid environments of Mars. The Qaidam Basin, the highest and one of the largest and driest deserts on Earth, is located in a dry, cold, and high UV environment, similar to the surface of Mars. We demonstrate a variety of landforms and also their counterparts on Mars, which include aeolian dunes and yardangs, polygons, gullies, valleys, and fluvial fans. In the Qaidam Basin, various environmental regimes for the formation of linear and asymmetric barchans have been described. Saline lakes and playas representing different stages of lake evolution in arid environment are also present in the Qaidam Basin and provide promising cases for studying the habitability in Mars-like environments. Results for microorganism isolation suggest that halophiles are the most important fraction in the hypersaline sediments and this may shed light on studying present martian habitability. Moreover, the remote but ready accessibility of the Qaidam Basin make it a potential site for engineering testing in regards to future martin exploration missions. We propose that the variety of exogenic and endogenic geomorphic types, lacustrine sediments, evaporite mineral assemblages and Mars-like extreme environments collectively point to the Qaidam Basin as an optimal

Key words: Aeolian landforms, desert, playa, astrobiology, analogue site, the Qaidam Basin, Mars

Introduction

Mars has been extensively morphologically and compositionally imaged by mission instruments onboard various orbiters, landers, and rovers, and at varying resolutions and spatial scales. The imaging instruments for morphology include: the High Resolution Stereo Camera (HRSC, (Jaumann et al., 2007), the ConTeXt camera (CTX, (Malin et al., 2007), the Thermal Emission Imaging System (THEMIS, (Christensen et al., 2004b), the High Resolution Imaging Science Experiment (HiRISE, (McEwen et al., 2007), and the Mars Orbiter Camera (MOC, (Malin and Edgett, 2001). The imaging instruments for composition include:the Thermal Emission Spectrometer (TES, (Christensen et al., 2001), Compact Reconnaissance Imaging Spectrometer for Mars (CRISM, (Murchie et al., 2007), Observatoire pour la Minéralogie, l'Eau, les Glaces et l'Activité (OMEGA, (Bibring et al., 2005), various in situ instruments were on landers and rovers (e.g., Vikings, Pathfinder, Spirit, Opportunity, Phoenix, and Curiosity) (Bell, 2008; Grotzinger et al., 2014). The results from these observations has revealed that the martian surface is rich in Earth-like geomorphologies; thus the study of terrestrial environments that are analogous to Mars has been listed as one of the highest priorities of Mars science investigations (Chapman, 2007; Farr, 2004; Greeley and Fagents, 2001; SpaceStudiesBoards, 2012), which includes habitability and life potential (Dohm et al., 2011; Dohm et al., 2004). With increasing new discoveries by in situ exploration, Mars exploration has begun to enter the era of focusing on detailed analysis at regional to outcrop level, rather than global mapping (Chapman, 2007; Farr, 2004). Analogue studies are playing a crucial role in this transition, on areas ranging from observation of surface geomorphology and composition to interpretation of their origin and formative processes.

Terrestrial analogue studies assist in helping to correctly understand the potential geological and possible biological processes operating on Mars (Bamsey et al., 2009; Binsted, 2015; Chapman, 2007; Dohm et al., 2011; Dohm et al., 2004; Farr, 2004; Garcia-Castellanos, 2007; Head and Marchant, 2014; Marchant and Head, 2007; Marlow et al., 2011; Romig et al., 2007). Interpretation of the diversity of landforms and their constituent materials on Mars (Carr, 2007; Clarke et al., 2006) requires many different counterparts as analogues on Earth, including

processes that form and modify surfaces in arid (e.g., aeolian, weathering, flood, mass-wasting, lacustrine, playa, evaporites) and polar regions (periglacial, ice and glaciers, permafrost, mass-wasting), and volcanic, tectonic, and impact processes in other regions. The presence of a wide variety of potentially habitable ancient environments on Mars (Dohm et al., 2011) also justifies investigations into their analogous environments and materials for biological studies on Earth (e.g., (Komatsu and Ori, 2000)). Previous studies have paid much attention to desert sites, where geomorphologies are similar to many of those observed on the martain surface, both from orbiting and in situ landing and roving spacecraft, and could provide clues to reveal information about the past climate and habitability of Mars. For instance, the Atacama Desert/Rio Tinto environments are examined to assess biology in extreme acidic environments and to search for biosignatures on Mars (Cabrol et al., 2007; Fernández-Remolar et al., 2008; Foing et al., 2011; Warren-Rhodes et al., 2007a; Warren-Rhodes et al., 2007b). The western US region (Baldridge et al., 2004; Chan et al., 2011, 2016), central Australia (Bourke and Zimbelman, 2001), and North Africa (Essefi et al., 2014a; 2014b; Paillou and Rosenqvist, 2003) are used to compare landforms and processes (e.g., yardangs, aeolian deposits, dry lake beds). Besides, arctic and polar regions are analyzed to examine the physical and biological processes related to cold, dry environments on Mars (Hauber et al., 2011; Head and Marchant, 2014; Levy et al., 2009; Marchant and Head, 2007; Osinski, 2007; Pollard et al., 2009). Furthermore, specific terrestrial analogue sites have been studied to provide insights into similar conditions on Mars, such as impact crater lakes (Komatsu et al., 2014), catastrophic flooding (Baker and Nummedal, 1978), and valley networks (Howard et al., 1987). Considering the present environmental conditions of Mars (e.g., dry, cold, high UV radiation, wind as the main force in modifying the surface, unidentified lifesignatures, etc.), however, the above Martian analogue sites do not cover all the environmental conditions. Thus, additional analogue sites are required to understand the far-reaching (in time and space) dynamic evolutionary history and environmental conditions. In this study, we introduce the unique geomorphological features of the Qaidam Basin, Tibetan Plateau, northwestern China and their martian counterparts.

The Qaidam Basin is the highest, and one of the driest and largest deserts on Earth (Rohrmann et al., 2013). It is characterized by extremely low precipitation, low annual temperature, high evaporation rates, and various aeolian geomorphologies, which is comparable to a dry and cold Mars (Fig. 1). In addition, high UV radiation and a variety of saline lakes, and evaporates in the region make it a candidate base for astrobiology, which includes the study of living forms adapted to harsh conditions similar to Mars and the preservation under extreme hyperarid conditions, etc. Several earlier studies focusing on evaporate sediments and mineralogy have suggested that the Qaidam Basin could potentially be a promising Mars analogue site (Kong et al., 2014; 2013b; Mayer et al., 2009; Wang and Zheng, 2009; Zheng et al., 2013; 2009). However, the Qaidam Basin offers a much wider range of study subjects for comparative planetology than previously outlined. In this study, we systemically introduce and provide preliminary assessments for the major geological, geomorphological, geochemical, and biological features and conditions that make the Qaidam Basin one of the best terrestrial analogue sites. These include: aeolian geomorphological features, distinctive evaporate sediments, evolutionary playas, saline lakes, and extremophiles in extreme climate and geological conditions. More detailed investigations of these features and application to Mars will be reported in future publications.

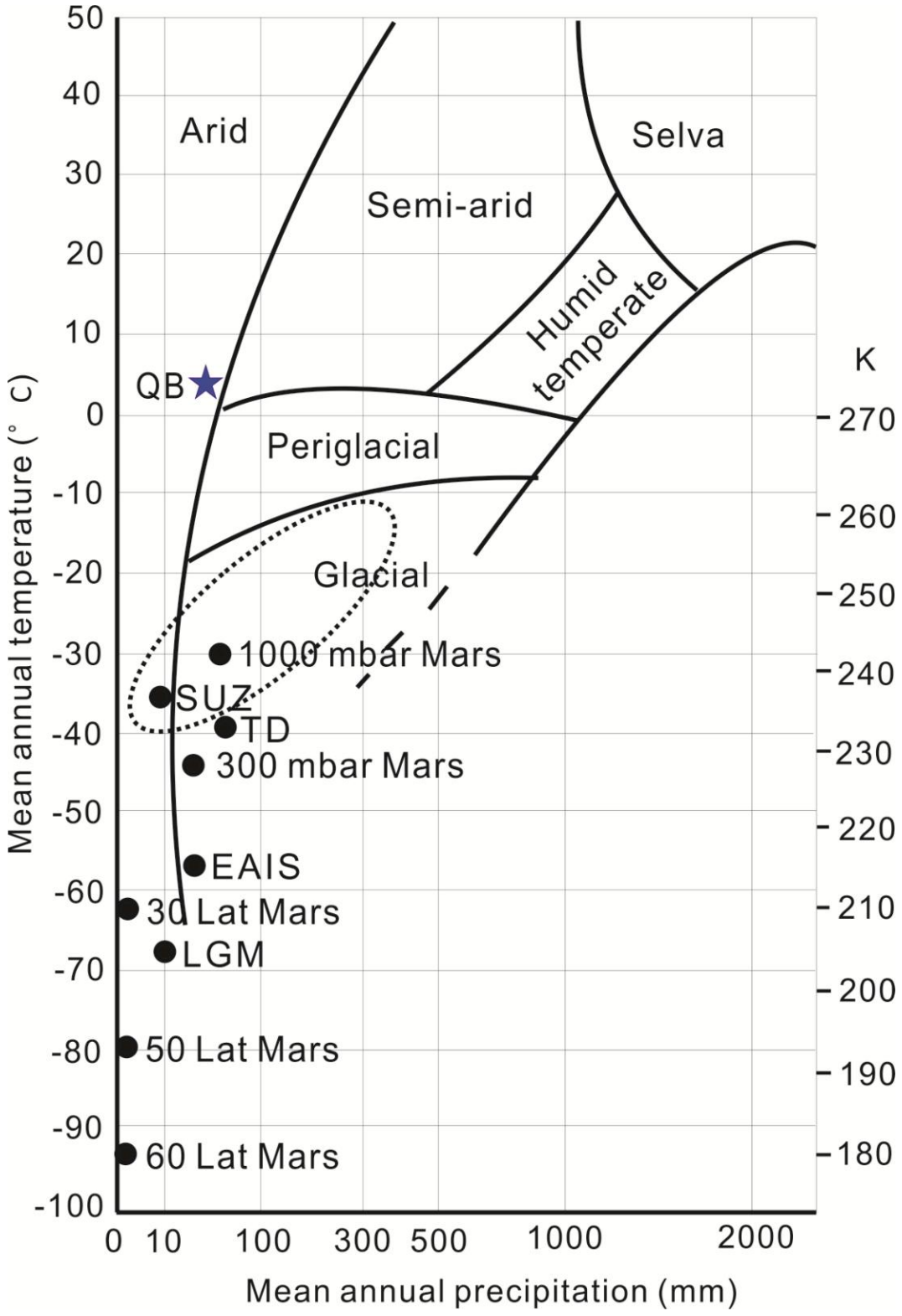

Figure 1. Morphogenetic regions for climate related landforms on Earth (adapted from Baker (2001) and Marchant and Head (2007)). The Qaidam Basin (QB) occurs in the arid region (shown as a star). Modern terrestrial glacial environments are plotted in the figure, including dashed oval for Antarctic Dry Valleys, TD for Taylor Dome, EAIS for Vostok, LGM for conditions during the

last glacial maximum (~18 ka) in interior East Antarctica. Modern Mars conditions at 30◦, 50◦, and 60◦ latitude are also plotted, as well as an ancient Mars at 300 and 1000 mbar.

1. Geological background and climate conditions

With an area of ~120,000 km^2 and an average elevation of ~2800 m, the Qaidam Basin is the largest sedimentary basin inside the 5000-m-high Tibetan Plateau, and the highest desert on Earth. It is surrounded by the Qilian orogenic belt to the northeast, the East Kunlun–Qiman Tagh orogenic belt to the south-southwest, and the Altyn Tagh Fault to the northwest (Fig. 2A). The basement of the basin is composed of Precambrian-Silurian metamorphic rocks that are overlain by Devonian-Cenozoic sedimentary strata (Huang et al., 1996). Recent magnetostratigraphic study suggests that the youngest sediments in the Huatugou area are ~11 Ma (Chang et al., 2015). The Cenozoic sediments within the basin are over 10,000 m thick, and consist mainly of saline to hypersaline lacustrine mudstone and siltstone, together with some fluvial sandstone and conglomerates at the margins (Rieser et al., 2005; Wu et al., 2012a; 2012b). The Qaidam Basin has been an internally drained basin since at least the Oligocene (Yin et al., 2008b). In response to the ongoing Indo-Asian collision, the basin is being shortened in a NE–SW direction since middle–late Miocene (Wu et al., 2014; Zhang et al., 2013), and its floor exposes folded, friable sedimentary rocks of the Miocene upper Youshashan, Shizigou and Qigequan Formations, which include many NW- to NWN-trending folds in its western part (Kapp et al., 2011; Wang et al., 2012).

The Qaidam Basin paleolake was a large single water body starting with its formation in the Jurassic, and then became many small lakes which resulted from fast uplift of the Tibetan Plateau and associated compressional deformation that resulted in an uneven basin floor during a relatively dry climate from the Miocene to the Pliocene (Yin et al., 2008a). Heterogeneous deformation and uplift of the Qaidam Basin caused the migration of the depositional center from west to east (Yin et al., 2008a). In the Oligocene, the depositional center was the Dalangtan depression and at that time the most ancient Dalangtan playa was formed. Subsequently, the depositional center migrated to the Kunteyi depression and finally shifted to Qarhan, which is

currently the largest saline lake and playa in the Qaidam Basin (Fig. 3B). The dominant evaporate salts at Dalangtan, Kunteyi, and Qarhan playas are sulfate, sulfate+chloride, and chloride, respectively (Kong et al., 2013b).

Today, being shielded by efficient orographic barriers, the annual precipitation in northwestern Qaidam Basin is less than 20 mm, and the annual aridity is ~ 50 (Sun et al., 1990), making it one of the highest and driest deserts on Earth (Rohrmann et al., 2013) 2015). With roughly one-third of the modern basin floor (~$3.88x10^4$ km^2) exposing yardangs carved in folded sedimentary strata, the Qaidam Basin is apparently dominated by deflation (Kapp et al., 2011; Zhou et al., 2006). Previous study has suggested that the erosion rates of sedimentary bedrock range from 0.05 to 0.4 mm/yr (Rohrmann et al., 2013). Strong winds, hyper-aridity, exposure of friable Neogene strata, and ongoing rock deformation and uplift in the western Qaidam Basin have created an environment where wind, instead of water, is the dominant agent of erosion and sediment transport.

The geological record, the associated landforms, and meterological observation, all suggest that the Qaidam Basin has been dry and cold both in the past and the present. The local meterological station at Mangya, Dalangtan playa, western Qaidam Basin has collected climate data for the past 30 years (from 1980 to 2011). The monthly average near surface air temperature ranged from maximum 16 ^oC in July to minimum -10.7 ^oC in January, and an annual average temperature of 3.5 ^oC. Also recorded were the annual mean value of relative humidity at 30 %, precipitation of which mostly occurred in June and July being 51 mm, the annual average evaporation equaling 2590 mm, an atmospheric pressure of 709 mbar, a monthly average wind velocity of 3m/s, and a monthly average sunlight of ~250 hrs (Kong et al., 2013a).

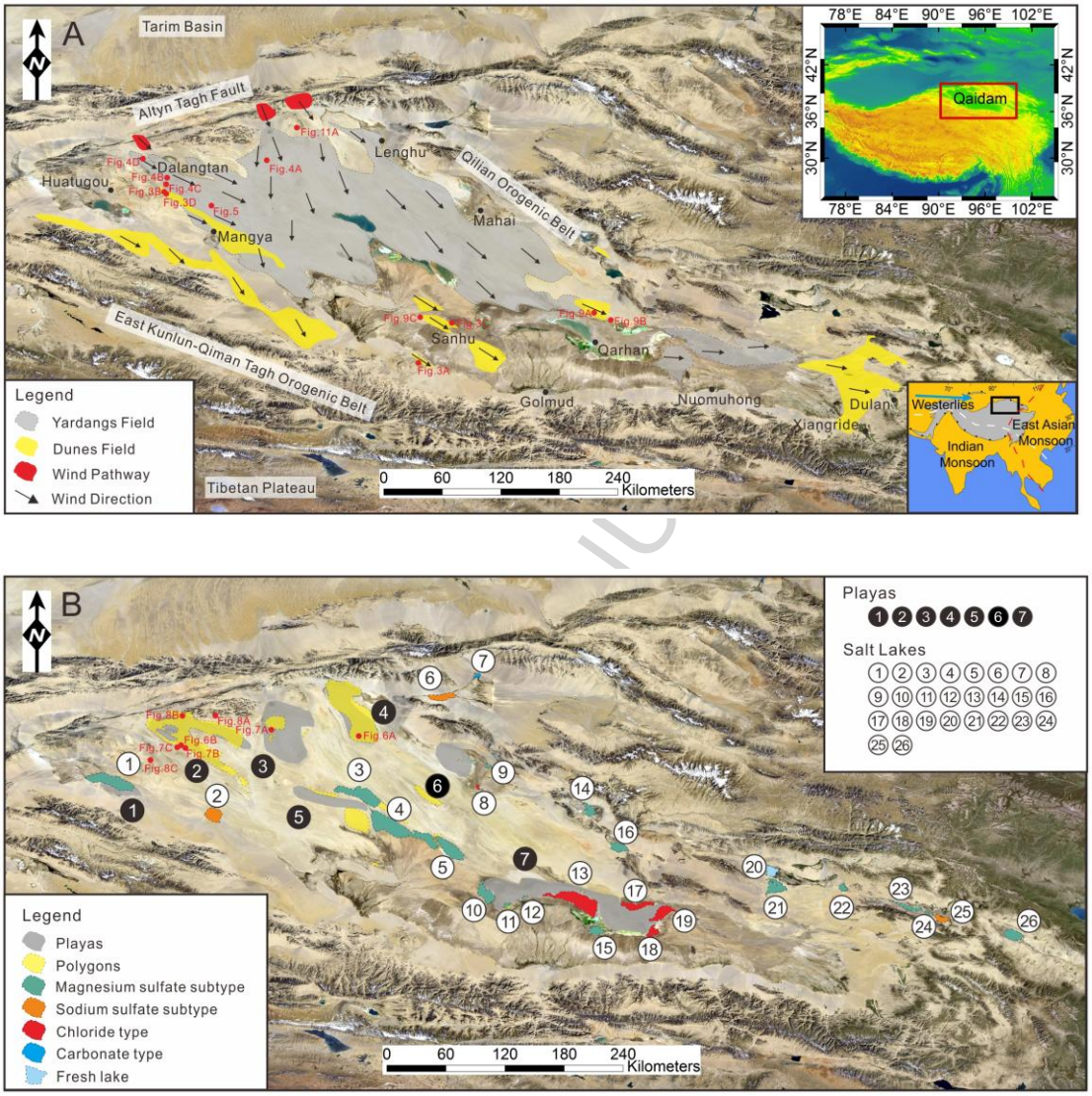

Figure 2. Main Mars-like geomorphologic landforms in the Qaidam Basin, NE Tibet Plateau. Base Image Credit: Google Earth. Inset map showing the location of Qaidam Basin is generated from 90 m SRTM data. (A) Aeolian landforms (modified after Kapp et al., 2011; Rohrmann et al., 2013); (B) Playas, polygons, and salt lakes in the Qaidam Basin. Playas are marked as: ❶Gasikule; ❷Dalangtan; ❸Qahansilatu; ❹Kunteyi; ❺Yiliping; ❻Mahai; ❼Qarhan. Lakes are marked as: ① Gasikule, ② Mangya, ③ Yiliping, ④ West Taijinaier, ⑤ East Taijinaier, ⑥ Dasugan, ⑦ Xiaosugan, ⑧ Balong Mahai, ⑨ Dezong Mahai, ⑩ Senie, ⑪ Dabiele, ⑫ Xiaobiele, ⑬ Dabuxun, ⑭ Daqaidam, ⑮ Tuanjie, ⑯ Xiaoqaidam, ⑰ Xiezuo, ⑱ South Huobuxun, ⑲ North Huobuxun, ⑳ Keluke, ㉑ Tuosu, ㉒ Gahai, ㉓ Qaikai, ㉔ Keke, ㉕ Xiligou and ㉖ Chaka. See text, Table 1 and Table 2 for details.

2. Geomorphology

A variety of Mars-like geomorphologies are well preserved within the Qaidam Basin, especially the desert regions, which cover a total area of ~ $9x10^3$ km^2 in the Qaidam Basin (Zeng et al., 2003). The most important ones are desert landscapes produced by wind and evaporation (e.g. dunes, yardangs, polygons, playas), gullies, valleys and saline lakes.

3.1 Dunes

Dunes are distributed mainly in three regions, the southwestern piedmont area, the Sanhu area, and the southeastern area of the Qaidam Basin (Fig. 2A, Yu et al., 2013). Previous studies of these three regions have included the investigation of geometric shapes (Hesp et al., 1989; Hu, 1990; Zhu, 1980), sediments (Bao and Dong, 2014; Bao and Dong, 2015; Qian and Liu, 1994), geochronology (Yu et al., 2015; Zeng et al., 2003), and formation and evolution histories (Yu et al., 2015; Zeng et al., 2003) of the dunes. In this region, dunes have been morphologically classified as barchan dunes, barchan dune chains, linear dunes, and star dunes (Liu et al., 2008; Xin, 1995; Zhu, 1980). Most of the dunes overlay well-bedded sediments. Barchan dunes are independently distributed, with widths and heights ranging from 50−300 m and 2−5 m, respectively. While their convex windward slope are gently dipping, and their concave leeward slopes steep (Fig. 3A), similar in shape and size to their counterparts on Mars (Fig. 3A').

Barchan dune chains are formed in areas rich in sand sources (Fryberger and Dean, 1979) and are usually several hundred meters to several kilometers long (Fig. 3B). Linear dunes mostly occur in the north part of the Qarhan Salt Lake and Sanhu areas (three lakes, namely east Taijinaier Lake, west Taijinaier Lake and Senie Lake). In some cases, the linear dunes co-exist with barchan dune chains and yardangs. Linear dunes at the northern Qarhan Basin are northwest trending (296^o), ~12 km long, 30−200 m wide, 5−30 m high, and 100−600 m apart. The linear dunes at the Sanhu area are also northwest trending (311^o) but relatively smaller in size (1−5 km long, 40−100 m wide, 3−20 m high, and 50−1400 m apart) (Fig.3C). Star dunes are rare with respect to other types in the Qaidam Basin (Fig. 3D). They are generally distributed among large barchan dune chains, forming due to the local multi-direction wind environment. On Mars, all of their analogs have been identified (Fig. 3A'; B', C', D').

We have found some brine water in the low-lying areas between the linear dunes in the north of Qarhan Salt Lake. Yu et al. (2015) proposed that the groundwater table is close to the surface, specifically less than 1 m depth in the relatively low-lyting plains that separate the linear dunes. Linear dunes in the Sanhu area also developed together with seasonal alluvial fans near the salt lakes.

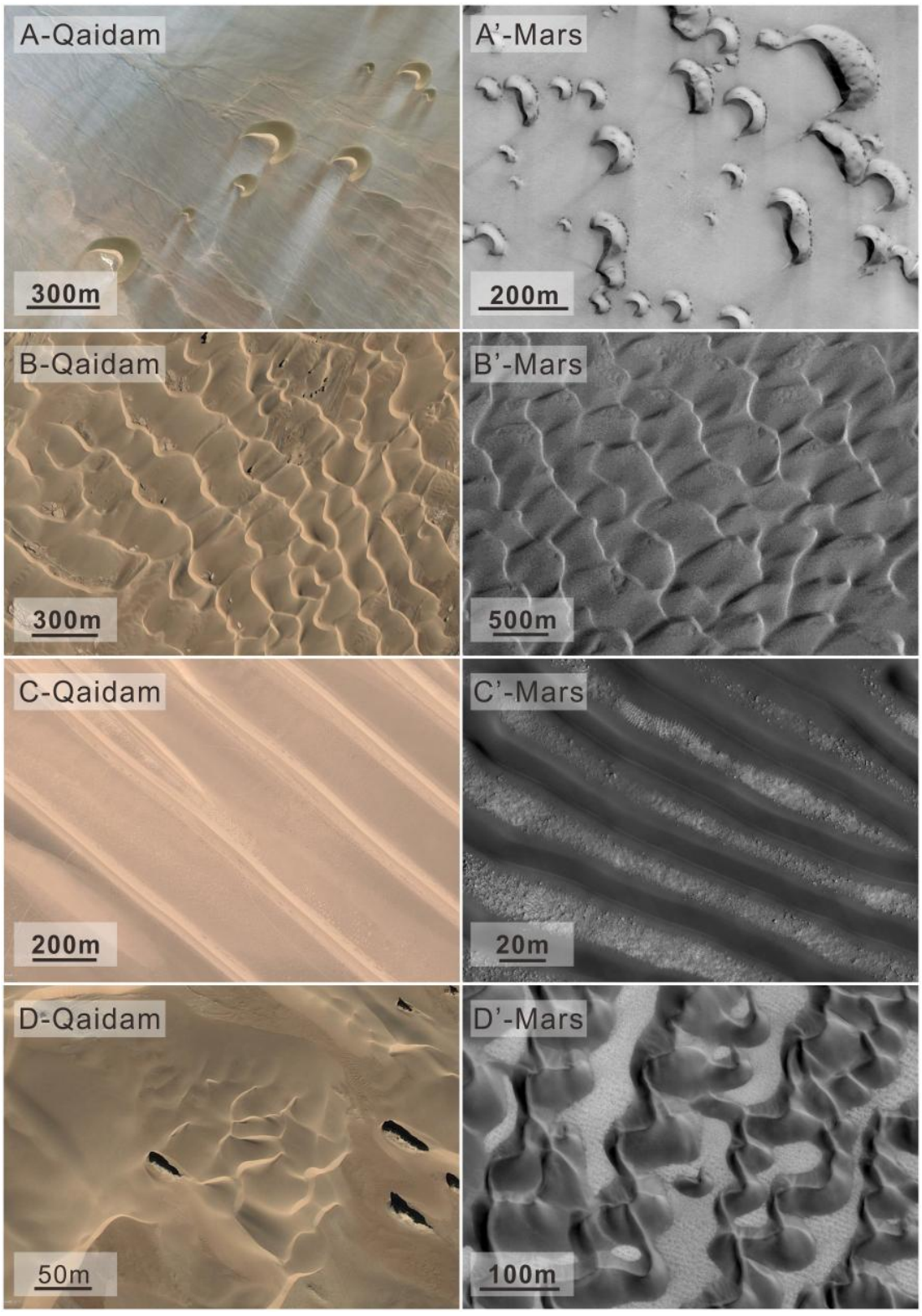

Figure 3. Various dunes in the Qaidam Basin and their counterparts on Mars. (A) Barchan dunes in the Qaidam Basin (image center: 36.663°N, 93.680°E). (A') Barchan dunes on Mars; portion of HiRISE image ESP_033228_2560_RED (image center: 75.748°N, 94.061°E). (B) Barchans dune chains (image center: 38.222°N, 91.363°E); (B') Barchans dune chains on Mars; portion of CTX image B21_017762_1891_XN_09N292W (image center: 9.12°N, 67.29°E). (C) Linear dunes

(image center: 37.002°N, 94.034°E). (C') Linear dunes on Mars; portion of HiRISE image ESP_0016036_1370_RED (image center: 42.660°S, 38.023°E). (D) Star dunes (image center: 38.222°N, 91.376°E); and (D') Star dunes on Mars; portion of HiRISE image ESP_018742_2565_RED (image center: 76.468°N, 297.450°E). All satellite images of the Qaidam Basin Credit: Google Earth.

3.2 Yardangs

Yardangs in the Qaidam Basin cover an area of ~3.88 x 10^4 km^2 (Kapp et al., 2011; Li et al., 2016; Liu et al., 2008) and thus it is the largest yardang region in China. These yardangs are mostly located in the northwest part of the basin (Fig. 2A, (Kapp et al., 2011; Rohrmann et al., 2013), and wind is the dominate erosional force for their formation (Kapp et al., 2011; Li et al., 2012; 2013). These yardangs show different sizes and shapes, and are classified into eight types (Halimov and Fezer, 1989; Li et al., 2016). In this study, we report the major yardang types (e.g., mesa, long-ridge, saw-toothed, remnant cone-like, ark-shape, and whaleback-like) and their Mars analogues in general.

Mesa yardangs are early-stage yardangs (Halimov and Fezer, 1989). They are mainly distributed in the continuum area of alluvial fan and the basin between the Mahai and Xiaoqaidam Lake. Mesa yardangs also developed in an area from Dafengshan to Chuanxingshan. These yardangs are usually irregular or elongated with a flat top and are large in scale,with lengths generally ranging from 200 m to several kilometers and heights reaching tens of meters.. Due to fluvial erosion, mesa yardangs have a less streamlined morphology, and sometimes have ambiguous orientations (Li et al., 2016). Long-ridge yardangs are well exposed in the Jianshan-E'boliang area surrounding the playa (Fig. 4A) and in the north of the Nuomuhong area. Yardangs in the Jianshan and E'boliang areas are usually 30−4 km long, and 7−200 m wide, with an interval distances of about 10−120 m. Some of them show a multi-layered structure, and part of their top layers have been eroded. While in the north of the Nuomuhong area, yardangs can be as long as 20 km with a 200−3000 m interval distance. Saw-toothed yardangs usually develop in the strata whose -dip direction is consistent with the local prevailing winds. They are generally oriented NW-SE and 2−20 m in height. Most of them are connected at their bases. Remnant

cone-like yardangs were formed by rapid erosion of saw-toothed yardangs (Halimov and Fezer, 1989). Whaleback-like yardangs are streamlined and appear like a whale back (or tadpole) when viewed from their side face (Fig. 4B). They are distributed in many places and typically occur in the Dalangtan playa area. Ark-shaped yardangs are widely distributed and are usually fusiform in satellite images, with steep windward heads (mostly with slope angles exceeding 60^{o}), and from side view, appearing as ark heads (Fig. 4O' in C). Their lengths generally range from several hundred meters to several kilometers, and their heights can reach 20 m .

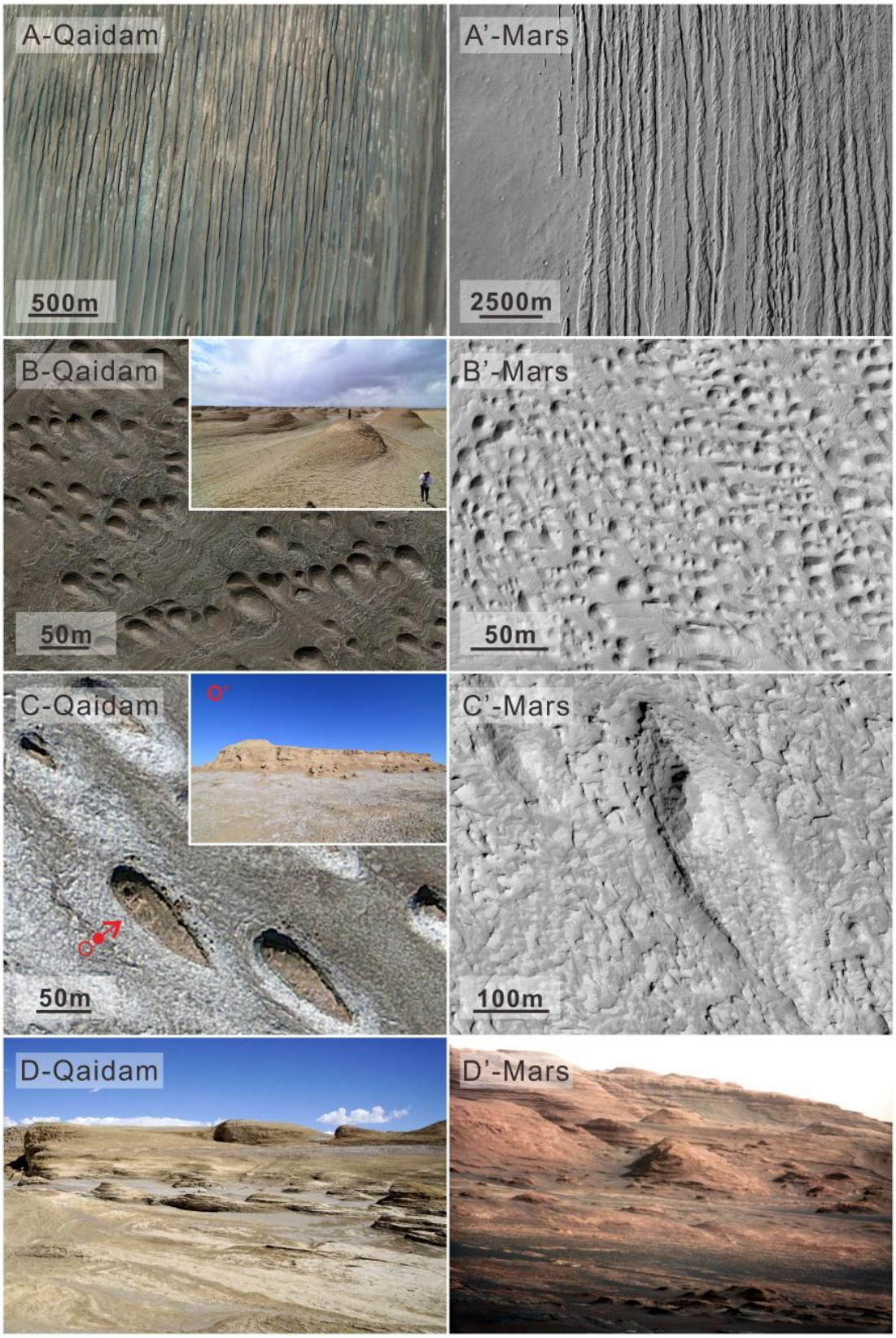

Figure 4. Typical yardangs in the Qaidam Basin and on Mars. (A) Long-ridge yardangs at the north of Jianshan (image center: 38.48°N, 92.28°E). (A') Long-ridge yardangs on Apollinaris Mons, Mars; portion of HiRISE image ESP_007671_1695 (image center: 10.461°S, 176.446°E).

(B) Whaleback-like yardangs in the Nanyishan area (image center: 38.402°N, 91.342°E). (B') Whaleback-like yardangs on Mars; portion of HiRISE image ESP_036510_1735 (image center: 6.612°S, 149.123°E). (C) Ark-shaped yardangs at the south of Nanyishan (image center: 38.12°N, 91.55°E), (O') Side view from point O in (C). (C') Ark-shaped yardangs in Aeolis Planum, Mars; portion of HiRISE image ESP_035231_1815 (image center: 1.350°N, 144.463°E). (D) Yardangs developed in lacustrine sediments (image center: 38.500°N, 91.162°E). (D') Yardangs in Gale Crater, Mars, imaged by the Curiosity Rover. All satellite images of the Qaidam Basin Credit: Google Earth.

We have also found that the occurrence of yardangs is controlled by sedimentary stratigraphy and wind direction. In Figure 5, the well-bedded stratigraphy and wind direction are noticeable. Yardangs are developed on relatively large grain-sized and rigid sediments, indicating that rock property is a major control factor for the formation of the yardangs.

Figure 5. Yardangs are controlled by both wind and stratigraphy.

3.3 Polygons

Polygonal surface structures (PSSs) are widespread surface phenomenon in the Qaidam Basin. They are mainly distributed inside seven playas (Gasikule, Dalangtan, Qahansilatu, Kunteyi, Mahai, Yiliping, and Qarhan) (Fig. 2B). On Earth, PSSs in the salt crust are interpreted to form by evaporation and crystallization of halite during the desiccation stage of the saline lake cycle (Lowenstein and Hardie, 1985). The diagenetic growth of salts within saline and mud layers beneath the dry lake surface leads to the disruption of saline crust into polygons (Christiansen,

1963). Generally, PSSs in the Qaidam Basin can be divided into three distinct types according to their sizes. The small-sized PSSs are commonly less than 10 m in diameter and mainly are seen as triangle, quadrangle, and hexagon shapes (Fig. 6A); their martian counterparts are shown in Figure. 6A'. Furthermore, there are some polygons spatially arranged along a line, appearing to be controlled by linear tectonic structures. Other typical PSSs, showing a lower interior floor and a relatively higher border, are closely assembled, forming a honeycomb texture in the Dalangtan playa (Fig. 6B). Figure 6B' shows the similar scale and shape of honeycomb polygons on Mars.

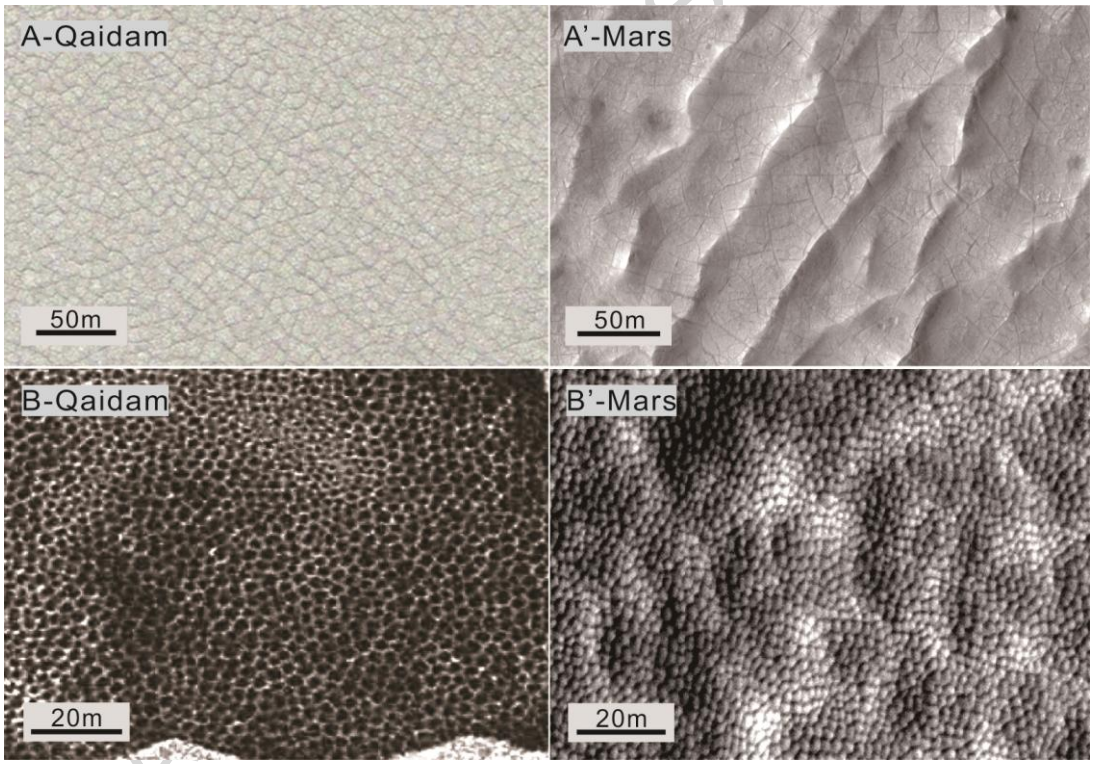

Figure 6. Small-sized PSSs in the Qaidam Basin and their counterparts on Mars. (A) Polygons appear to be arranged along a line. Image center: 93.06°E, 38.47°N, marked with P2 in Figure 1b. (A') Small-sized polygons formed on a chlorite-bearing material on Mars (image center: 220.98°E, 38.81°S); portion of HiRISE image PSP_003160_1410_RED. (B) Honeycomb polygons in the Qaidam Basin, image center: 91.52°E, 38.43°N. (B') Honeycomb landforms in the Pavonis Mons caldera on Mars; portion of HiRISE image PSP_002249_1805. All satellite images of the Qaidam Basin, Credit: Google Earth. North is up in all figures.

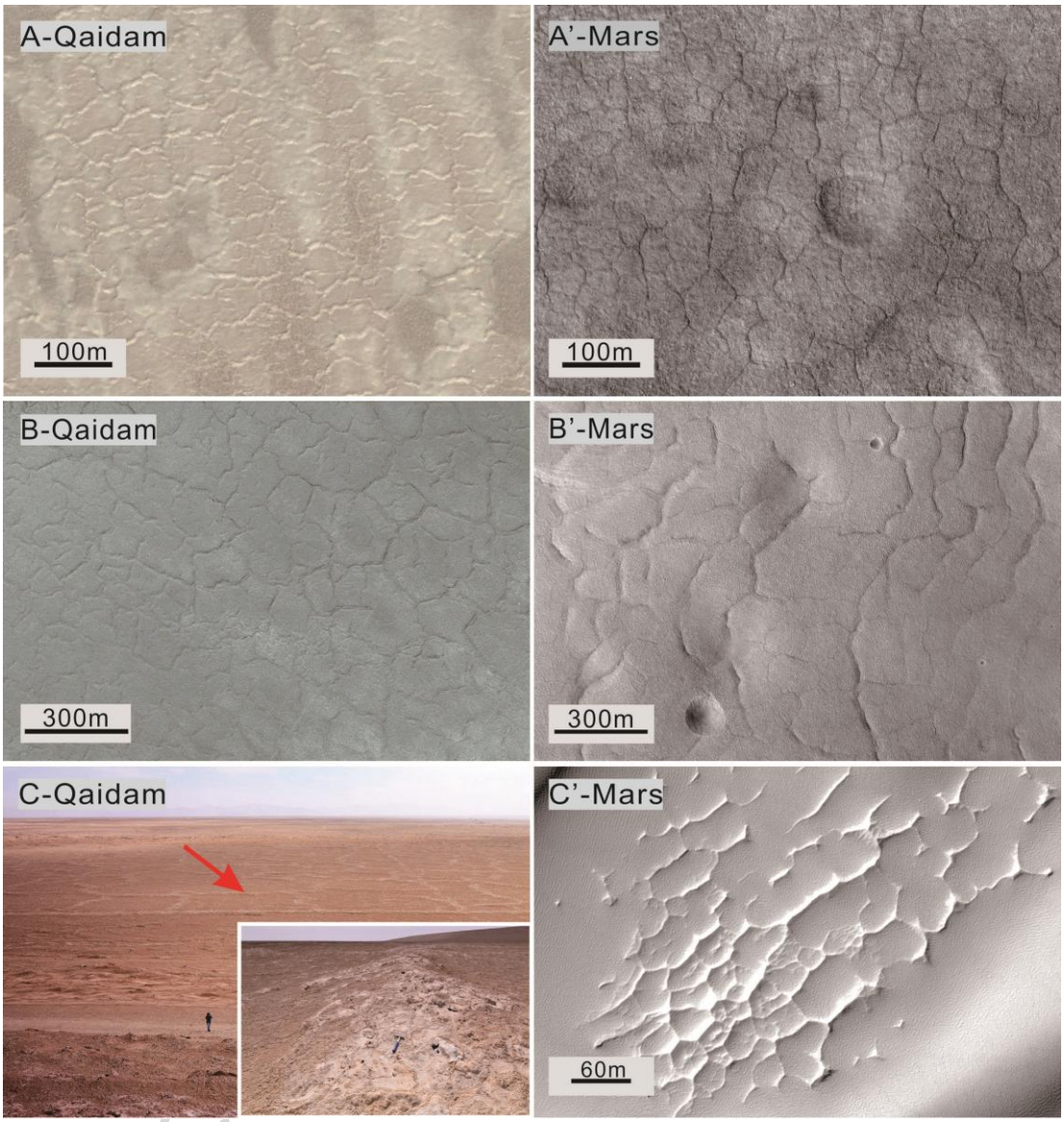

Figure 7. Middle-sized and large-sized PSSs in the Qaidam Basin and their counterparts on Mars. (A) Middle-sized polygons with discontinuous borders in the Qaidam Basin (image center: 92.40°E, 38.56°N). (A') Middle-sized polygons in Utopia region, Mars; portion of HiRISE image PSP_001938_2265_RED (image center: 92.11°E, 46.04°N). (B) Large-sized polygon examples seen in the Qaidam Basin (image center: 91.53°E, 38.40°N). (B') An example of large-sized polygons in a crater floor in Acidalia Planita, Mars (image center: 341.61°E, 50.70°N); portion of HiRISE image PSP_001942_2310_RED. (C) Large-sized PSSs photographed during the field investigation, with a man is shown for scale at the bottom of the figure. The inset picture shows the enlarged view of a raised rim of a large-sized PSS, with a hammer shown for scale. Image acquired in July 2015 (C') Raised rim PSSs in the Roddy Crater floor, Mars (320.32°E, 21.77°S); portion of HiRISE image ESP_034750_1580_RED. All satellite images of the Qaidam Basin, Credit: Google Earth. North is up in all figures.

Middle-sized PSSs (10–100 m) in the Qaidam Basin exhibit a significant variation in appearance. Some PPSs of this size have discontinuous subdued borders, possibly caused by other processes such as aeolian erosion (Fig. 7A); similar-sized PSSs on Mars are shown in Figure. 7A'. Most of these are located in the Qarhan, Qahansilatu, Mahai, and the northern region of the Dalangtan playa. Of these middle-sized PSSs in the Dalangtan playa, some have elevated ~10-m-in-wide borders with respect to their surroundings. In many cases, they contain relatively small polygons. The coexistence of middle-sized PSSs and yardangs is also seen in some places such as the Qarhan playa.

Large-sized PSSs (100–300 m) commonly appear at the outer edge of the Dalangtan playa. According to previous studies of Earth polygons, the slow lowering of ground-water levels and episodes of intense evaporation were proposed to be responsible for the formation of large-sized PSSs (El Maarry et al., 2012; T Neal et al., 1968). They display different forms and have borders that vary in width from 4 m to 6 m. In addition, small-sized PSSs are often seen in their inner surfaces. It should be noted that the large-sized PSSs at the foot of the Nanyishan in the Dalangtan playa have raised borders with side lengths varying from 20 m to 150 m (Fig. 7B). Figure 7B' shows the large-sized crater floor polygons (with average size of 120 m) on Mars (El Maarry et al., 2010), which show similar features and size as those in the Dalangtan playa.

Field investigation showed that PSSs in the Qaidam Basin range from centimeters to hundreds of meters in diameter (Figs. 6 and 7), and most of them have raised rims. Field measurements revealed that these rims are several centimeters to ten meters in width and tens centimeters up to two meters in height. For example, a rim of a large-sized polygon in the Dalangtan playa exhibits a broad arch with a rugged top surface (Fig. 7C). Near its top center, pores, vents, and depressions suggest the existence of subsurface voids (the inset picture in Fig. 7C). It is common to see stalactite-like halite crystals when the top masses are turned over. Importantly, a top center fracture can be seen for some arched rims. Raised-rim PSSs are also seen on some martian crater floors, such as Roddy Crater (Fig. 7D).

3.4 Gullies, fluvial valleys, and alluvial fans

A gully is defined as a steep-sided channel, often with a steeply sloping and actively eroding head scarp (Bocco, 1991; Poesen et al., 1996). Gullies in the Qaidam Basin can be tens to hundreds of meters long and usually form on hillsides during or after heavy rains (Fig. 8A). However, light rain or small water flow can also develop gullies when it the water runs through loose sands.

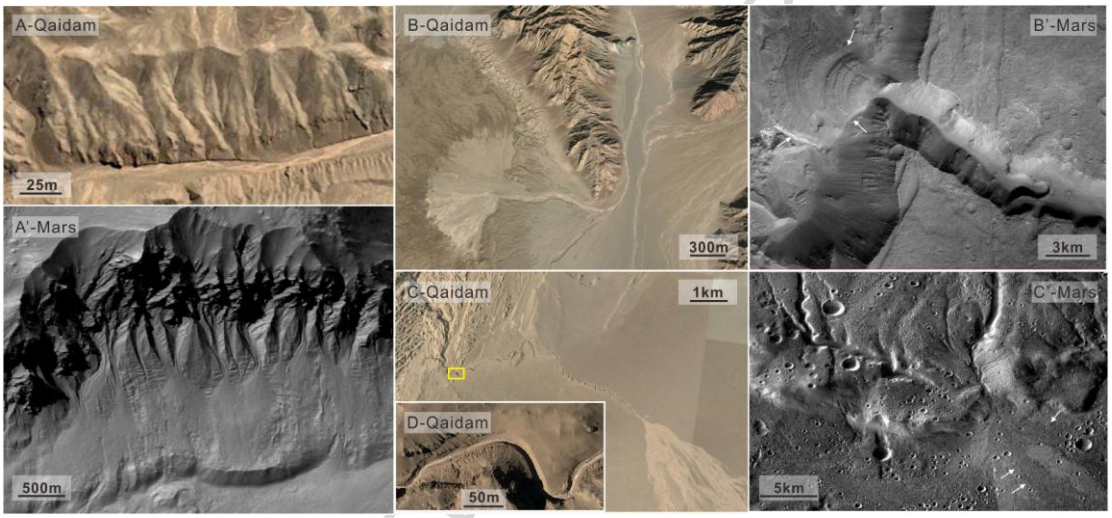

Figure 8. Gullies, valleys, and alluvial fans in the Qaidam Basin and their counterparts on Mars. (A) Gullies in the Qaidam Basin (image center: 38.67°N, 91.84°E,). (A') Gullies in Hale Crater, Mars; portion of CTX image D15_033115_1430_XI_37S036W (image center: 34.58°S, 323.14°E,). (B) The first type of valleys and associated alluvial fan (image center: 38.72°N, 91.52°E). (B') The martian counterpart of the valley and alluvial fan (white arrows) in (B'); portion of CTX image D08_030518_1650_XN_15S060W (image center: 299.72°E, -15.07°N). (C) The second type of valley and its associated alluvial fan (image center: 38.30°N, 91.27°E). Yellow box denotes the location of (D). (C') The martian counterpart of the valley and alluvial fan (white arrows) in (C); portion of CTX images P22_009474_1378_XN_42S091W, B21_017766_1536_XN_26S035W, and B05_011531_1378_XI_42S091W (image center: 42.97°S, 268.72°E). (D) Enlarged image of the valley in (C) (image center: 38.28°N, 91.27°E). All satellite image of the Qaidam Basin Credit: Google Earth.

Fluvial valleys of different scales are widely distributed in the Qaidam Basin, especially in the marginal area of the basin. Most of them originate from the surrounding mountains and are formed by glacial melt water and occasional rainfall (Kong et al., 2014; Zhang and Liu, 1985). The morphology of the valley networks is diverse and can be divided into two main morphologic types. The first type has a low sinuosity and exhibits relatively shallow erosion depths (i.e., meters

or less). This type of valley usually originates from mountains with granitic bedrock. For example, the fluvial valley in Figure 8B originates from the mountain formed of Caledonian and Hercynian granitoid intrusions. The maximum width of the main stream is about 110 m, but the depth is less than 1 m. The other type has a high sinuosity and is deep (Fig. 8D). This type usually originates from mountains consisting of sand-mudstone (Fig. 8D). The maximum valley width is about 150 m, the width of the main stream less than 20 m, and the depth can reach 15 m. In high-resolution remote sensing images (Fig. 8D), the valleys display V-shaped cross-section and deeply incise into the sedimentary layers.

Alluvial fans are common features that develop at the end of valleys. In the Qaidam Basin, there are two main types of alluvial fans: apron-shaped and elongate. In Figure 8, typical alluvial fans of these two types can be seen. The apron-shaped alluvial fan in Figure 8B covers an area of ~0.7 km^2. Its radius is ~0.7 km, and the elevation difference between the top and the bottom of the fan is 20 m. The elongate fan in Figure 6C extends for more than 5 km, and the elevation difference is 70 m. It covers an area of ~8 km^2. On Mars, fans with similar morphology can also be found at the end of some valleys (Fig. 8B' &C').

3.5 Playas and evaporates sediments

Quaternary evaporite deposits are well preserved in the seven playas (Wang et al., 2013b). However, these playas were formed at different times and had distinct physic-chemical evolution histories. At the end of the Pliocene, great changes occurred in the evolution of the saliferous lakes of the Qaidam Basin. As the tectonic uplift migrated from west to east since late Pliocene, the Kunteyi, Qahansilatu, Dalangtan lakes changed to playas by the late Pleistocene, and the Mahai, Yiliping, and Qarhan playas formed approximately at 15,000–9000 yr B.P. (Chen and Bowler, 1986).

Since the arid environments and controlling geochemistry have differed from basin to basin through time, the composition of the salt minerals and thickness of salt deposits have also varied across the region (Chen and Bowler, 1986; Huang et al., 1993). generally, sulfate-rich evaporites such as gypsum occur in the Gasikule, Kunteyi, Qahansilatu and Dalangtan playas in the western

region, while halite with a ralatively low sulfate content occurs principally in the Mahai, Yiliping and Qarhan playas in the eastern region (Chen and Bowler, 1986). The Yiliping playa lies at the boundary between deposits of different composition. The thickness of salt in the west is usually more than 100 m compared to an average about 20–40 m and a maximum of 73 m east of the Yiliping playa (Huang et al., 1993).

The Dalangtan playa, located in the northwestern region of the Qaidam Basin, was the major depositional center of the basin in the Pliocene, estimated to have been approximately 44 km long and 6-15 km wide (Shen, 1993). The entire basin floor is entired covered by evaporative salty crusts.. Generally, Neogene and Quaternary sediments occur widely in the basin. There are hundreds of-meters-thick evaporates with a dominance of sulfates deposits (Milly et al., 1993; Zheng et al., 1993). The characteristics of seven major playas within the Qaidam Basin are listed in Table 1, which formed earlier, have more complex evaporite mineral assemblages and there are only a few salt lakes remaining within the youngest Qarhan playa region (Fig. 2B).

Table1. Characteristics of major playas within the Qaidam basin (Wei et al., 1992; Zheng et al., 1993; Zheng et al., 2002a).

No	Playa	Center coordinates	Area (km^2)	Salt deposition thickness (m)	Elevation (m)	Evaporite minerals
1	Gasikule	91°55′E 37°05’N	140	300	2850	Halite, carnallite, sylvine, mirabilite, glauberite, gypsum, bloedite, epsomite, hexahydrite, leonhardtite
2	Dalangtan	91°29′E 38°29’N	500	417	2695	Halite, carnallite, sylvine, kainite, picromerite, mirabilite, syngenite, epsomite, hexahydrite, leonhardtite
3	Qahansil	92°26′E	2000	452	2700	Halite, mirabilite,

	atu	38°09’N				glauberite, gypsum, bloedite, carnallite, ulexite, borax
4	Kunteyi	93°05′E 38°50′N	1680	300	2724	Halite, mirabilite, glauberite, antarcticite, carnallite, epsomite, gypsum
5	Yiliping	93°05′E 37°58’N	360	200	2683	Halite, epsomite, carnallite, gypsum
6	Mahai	94°10′E 38°20′N	2000	198	2743	Halite, mirabilite, epsomite, carnallite, ulexite, borax
7	Qarhan	95°15′E 36°55′N	5856	73	2677	Halite, carnallite, sylvine, bischofite, gypsum, antarcticite, polyhalite

4 Saline lakes

The Qaidam Basin experienced a long geological history, responding to the uplift and deformation of the Tibetan Plateau. The basin began to accumulate continental deposits from river systems starting in the Jurassic period, and an ancient lake formed in the early Tertiary (Chen and Bowler, 1986). From the late Miocene to the early Pliocene, the ancient lake expanded and migrated from the northwest to the southeast due to more rapid uplift in the northwestern part of the Qaidam Basin. Then the ancient lake was divided into several secondary lakes and most of them underwent desiccation to become playas due to tectonic movements and climate change (Chen and Bowler, 1986). Today, only several small lakes contain standing water. Most of them lie along the front of the Kunlun Mountain and Qilian Mountain, and are located in the center part of the basin, aligned in a NW-SE direction (Fig. 2B).

Among the twenty-six modern and paleolakes, Keluke is the only fresh lake; the other twenty-five lakes are saline lakes (Fu, 2008; Zheng, 1997; Zheng et al., 2002a). However, the salinity of the Keluke lake, 0.7 g/l (Yang, 2013), could be treated as a saline lake as well. The common ions in the saline lakes are Ca^{2+}, Na^{+}, Mg^{2+}, K^{+}, Cl^{-}, SO_4^{2-}, CO_3^{2-} and HCO^{-}. The saline

lakes were divided into three types based on their hydrochemical characteristics (i.e., the main ions) (Zheng and Liu, 2009). They are the chloride type (including Balong, Mahai, Dabuxun, and Xiezuo lakes), the carbonate type (Xiaosugan lake), and sulfate type with two subtypes as magnesium sulfate subtype (e.g., Gasikule, Kunteyi Senie lakes), and the sodium sulfate subtype (Dasugan, Mangya and Xiligou lakes). The general characteristics of most saline lakes within the Qaidam Basin are listed in Table 2.

Table 2. General characteristics of salt lakes in the Qaidam Basin.

No.	Name	Center Coordinate	Area（km^2）	Altitude (m)	Hydrochemical Type	Degree of Mineralization (g/l)	pH
1	Gasikule	90°55'E, 38°04'N	103	2853	magnesium sulfate [1]	333.2 [3]	7.6 [3]
2	Mangya	91°50'E, 37°46'N	2	2886	sodium sulfate [3]	41.4 [3]	8.7 [3]
3	Yiliping	93°09'E, 38°59'N	360	2863	magnesium sulfate [3]	327.2 [3]	7.3 [3]
4	West Taijinaier	93°22'E, 38°43'N	82	2678	magnesium sulfate [1]	336.3 [3]	7.7 [3]
5	East Taijinaier	93°55'E, 37°30'N	116	2681	magnesium sulfate [3]	331.5 [3]	7.7 [3]
6	Dasugan	93°55'E, 37°30'N	104	2850	sodium sulfate [4]	25~32 [5]	9.7 [7]
7	Xiaosugan	94°12'E, 39°01'N	12	2691	carbonate [4]	1.2 [5]	9.5 [7]
8	Balong Mahai	94°13'E, 38°02'N	5	2743	chloride [3]	313.9 [3]	7.4 [3]
9	Dezong Mahai	94°19'E, 38°14'N	11	2740	magnesium sulfate [3]	355.2 [3]	7.4 [3]
10	Senie	94°19E, 37°03N	69~85	2676	magnesium sulfate [1]	332.2 [3]	7.1 [3]
11	Dabiele	94°31E, 36°59N	7	2677	magnesium sulfate [3]	362.9 [3]	7.0 [3]
12	Xiaobiele	94°39'E, 37°02'N	6	2677	chloride [1]	386.9 [3]	6.2 [3]
13	Dabuxun	95°06E, 36°58N	184~334	2765	chloride [1]	307.6 [this study]	7 [this

							study]
14	Daqaidam	95°10'E, 37°50'N	23~36	3148	magnesium sulfate [1]	274.4 [3]	7.9 [3]
15	Tuanjie	95°21′E, 36°48′N	6	2673	magnesium sulfate [1]	425.3 [3]	5.4 [3]
16	Xiaoqaidam	95°30'E, 37°31'N	36~40	3147	magnesium sulfate [3]	131.08 [this study]	8.83 [this study]
17	Xiezuo	95°39E, 37°00N	17	2696	chloride [1]	358.5 [3]	5.5 [3]
18	South Huobuxun	95°47E, 36°44N	33	2670	chloride [1]	346.1 [3]	6.7 [3]
19	North Huobuxun	95°55E, 36°54N	51~90	2676	chloride [1]	306.8 [3]	6.7
20	Keluke	96°55E, 37°18N	58	2812	/	0.7 [this study]	8.8 [this study]
21	Tuosu	96°57E, 37°04N	166	2808	magnesium sulfate [2]	29.1 [this study]	8.8 [this study]
22	Gahai	97°33E, 37°08N	37	2851	magnesium sulfate [3]	66.58 [this study]	8.35 [this study]
23	Qaikai	98°01E, 37°01N	18	2940	magnesium sulfate [3]	324.1 [3]	6.9 [3]
24	Keke	98°14E, 36°58N	4	3010	magnesium sulfate [3]	326.4 [3]	6.8 [3]
25	Xiligou	98°27E, 36°50N	20	2938	sodium sulfate [3]	213.3 [3]	7.6 [3]
26	Chaka	99°07E, 36°33N	104	3059	magnesium sulfate [1]	337.86 [this study]	7.56 [this study]

Noted: Data were collected from [1] (Yu, 1984); [2] (Wang et al., 1998); [3] (Zheng et al., 2002b); [4] (Fan et al., 2007) [5] (Hou, 2010).

[this study]: average values of measured in 2010, 2013, 2014, 2015, and 2016. These data were analyzed at the Key Laboratory of Biogeology and Environmental Geology (China University of Geosciences, Wuhan, China) by Prof. Hongcheng Jiang.

"/" in the table means unavailable data.

As listed in Table 2, most lakes were alkaline, with pH values ranging from 7 to 9. However, there have been eight acid lakes indentified: (named Xiaobiele, Dabuxun, Tuanjie, Xiezuo, South Houbuxun, North Huobuxun, Qaikai, and Keke) (Fig. 2B). All of them are distributed in the eastern part of the Qaidam Basin (Xiaobiele Lake was seen on the boundary here). In addition, among the five chlorite-type lakes, four of them are located in the east part of the Qaidam Basin. According to previous studies, tectonic movements associated with climate change had contributed to the northwestuplift and associated water supply that fed the river system that debouched into the eastern part of the basin. Thus, evaporation began in the northwestern region, then later occurred in the southeastern region. As more soluble chloride more easily migrated than sulfate and carbonate, , chloride became concentrated in the lake terminus, which is located in the Qarhan region (Chen and Bowler, 1986). Three chloride-type lakes (i.e., Xiezuo, South Huobuxun and North Huobuxun) were located in the Qarhan region (Fig. 2B), which is the lowest part of the Qaidam Basin.

The degree of mineralization of most lakes ranges from 200 g/l to 450 g/l. Only four lakes, Mangya, Dasugan, Xiaosugan, and Gahai, have a mineralization degree lower than 100 g/l (Table 2). The data suggest that mineralization degree has an inverse relationship with pH values. The higher the mineralization presented, the lower the pH values displayed.

5 Habitability

The Qaidam Basin is not an eco-friendly region due to its high altitude, dry, cold, and high UV radiation environment. The most extreme environments in the region are playas and hypersaline lakes, where vegetation is sparse to non-existent and life (including plants, animals, and insects) is not visible.. However, some kinds of microorganisms could thrive in these extreme habitats (Kong and Ma, 2010). Thus, numerous playas and saline lakes within the Qaidam Basin provide ideal materials to study microbial communities and their metabolic activity via both molecular techniques and culture-dependent methods in hypersaline environments. With microbial experiments, culturable microbes isolated from the hypersaline deposits could enrich our understanding of the microbial diversity in this region. Extracting biomolecules preserved in

the sediments would help in the understanding of the local geological record of life (Seewald, 2001).

Lipid molecules have been found in saline lakes and most results suggest that salinity is the main factor influencing the microbial community (Jiang et al., 2007; Wu et al., 2006). It was proposed that *Betaproteobacteria* favor freshwater environments while *Alphaproteobacteria* and *Gammaproteobacteria* are mainly detected in hypersaline water conditions of the Qaidam Basin (Wu et al., 2006). By analyzing a 900-cm hypersaline sediment core from the Qaidam Basin, (Jiang et al., 2007) found that the bacterial community was dominated by halophilic and halotolerant bacteria, and halobacteriales of the euryarchaeota was the major group in the hypersaline sediments.

Lipids biomarkers are widely used in the fossil record to determine the source organisms as they have high preservation potential. Even in the case of digenetic alteration, lipids may still maintain sufficiently well-preserved basic structures, which allow the recognition of their original compounds and biological precursors (Seewald, 2001). Wang et al. (2013a) found that halophiles were the most important archaea in the hypersaline sediments of the Qaidam Basin, as they are thought to be the producer of archaeol. In our preliminary study, we identified and quantified lipids extracted from evaporite sediments collected from the Dalangtan playa, which is the driest region in the Qaidam Basin. We examined the concentration and distribution of fatty acids synthesized by bacterial, and acyclic diether and tetraether membrane lipids synthesized by archaea. Bacterial and archaeal biomolecules have been detected in the different depositional units. Our results show that the abundance of microbial derived compounds varies with different salinity units; that is archaeal lipids dominate in units with high salinity, whereas bacterial lipids become dominant in detrital units with low salinity.

Microbial study of the Dalangtan playa has been reported by (Kong and Ma, 2010). They sampled salt crusts and other sediments in the Dalangtan playa, and isolated strains of *Virgibacillus*, *Oceanobacillus*, *Terribacillushalophilus*, *Halobacillus*, *Streptomyces*, and *Acinetobacter*. To verify these results and know better their correlation with mineral assemblages

and environment, we further conducted microbial isolation from evaporate sediments of the Dalangtan playa. The mineral compositions of the collected samples were conducted using X-ray diffraction, and analyzed with software X-Powder (http://www.xpowder.com/) and JADE (http://materialsdata.com/). The results suggested that surface samples are dominated by chlorides with a slight amount of gypsum, while subsurface samples (~ 7 m in depth) are composed of chlorides, gypsum, carbonates, clays (illite, smectite, chlorite etc.), quartz, and feldspar. The pH values were measured with a pH meter (UB-7 DENVER, America), and the pH values are from 7 to 9. Moisture contents range from as high as 12.45 wt%, to as low as 0.33 wt%; these were tested with freeze drying equipment (ALPHA 1-2 LD, Martin Christ, Germany) for 24 hrs at the Key Laboratory of Biogeology and Environmental Geology (China University of Geosciences, Wuhan, China).

Regarding microbial analysis, modified growth media (MGM) (Dyall-Smith, 2009) were used to isolate microbes from the samples. The microbes in the Dalangtan playa have very long adjustment periods in the laboratory environment, usually taking one month or so to adjust themselves until they grow into a colony on the agar plates. Twenty-three strains of bacteria and seven strains of fungal species have been isolated from the deposits. Identification of microbial isolates was done with molecular analysis of 16S rRNA and ITS1 for bacteria and fungi respectively. For DNA extraction and Polymerase Chain Reaction amplification of the isolates were referred to Man et al. (2015) and Yun et al. (2016). Sequencing was conducted by Tianyi Huiyuan Bio-Technique Co. Ltd., Wuhan, China for bacteria and GenScript, Nanjing, China for fungi. Phylogenetic analyses were conducted with MEGA6 (Tamura et al., 2011). The results suggest that bacteria show more than 97% similarity to *Bacillus*, *Oceanobacillus*, *Thalassobacillus*, *Gracilibacillus*, *Nocardiopsis*and, and *Halobacillus*belonging to three orders (Bacillales, Micrcoccales, and Streptosporangiales) of two phyla (Firmicutes and Actinobacteria). Among these, *Bacillus* were major species and accounted for 45%. Sequenced fungi show more than 97% similarities to *Phialosimplex*, *Chaetpmium*, and *Aspergillus*, belonging to three orders (Eurotiales, Capnodiales, and Sordariales) of one phyla (Ascomycota). Growth curves of four strains of microbes (i.e., Thalassobacillus sp., Ocenobacillus sp., Ornithinibacillus sp., and

Halobacillus sp.) in MGM media were monitored by measuring the optical density (OD 600) of the cultures every 24 hours by ultraviolet and visible spectro-photometer (TU-1800, PERSEE, China). The relatively premium salinity for growth of *Oceanobacillus* and *Halobacillus*is is about 15%, while that for *Thalassobacillus* and *Ornithinibacillus* is about 12%. According to these experiments, *Bacillus* is the most abundant species among the isolates.

6. Discussions

6.1 Dunes and yardangs

Dunes and yardangs are typical landforms resulting from wind- and/or water-erosion, transportation, and deposition (Kapp et al., 2011; Ward et al., 1985). Active dunes are representatives of present-day surface wind regimes in desert regions (wind direction and its variation with time, wind force, local landform and sand properties, etc.; Bridges et al. 1999; Greeley et al., 2003; Bourke, 2010). The different types of dunes are controlled by the specific wind field (Edwin D, 1979; Fryberger and Dean, 1979; Tchakerian, 1995; Zeng et al., 2003). Dunes are also widely distributed on Mars (Bourke, 2010; Cardinale et al., 2012; Carr, 2007; Greeley et al., 1981; Hayward et al., 2007), and their present-day motions have been measured at some localities (e.g. (Bridges et al., 2012; Cardinale et al., 2016)) indicating that they are still active landforms. However, there is very limited meteorological data on Mars, and ground-based meteorological data are only available for four sites on the planet and cover very short time periods (Bourke, 2010), so we know little about the actual wind regime at the local scale and their significance on atmosphere circulation at global scale of Mars. In this case, the dunes on Earth could serve as an indicator of the interaction between the atmosphere and the surface (Hayward et al., 2007). Their orientations, morphologies, and movements may be used to infer aspects of the wind environments in which they were formed (Sefton-Nash et al., 2014). They also have the potential to be applied as a proxy for formative wind regimes and sand supply (Bourke and Goudie, 2009). The affinity of types and sizes of dunes in the Qaidam Basin and on Mars (Fig. 3) provides an opportunity to learn how wind works in these planetary environments, and the source and sink relationships on the martian surface.

Also, the base of sand dunes and later solidification of their surface may play important roles on the formation of different dune shapes, even in the same wind regime condition. For instance, linear duns are commonly regarded as resulting from bi-directional wind operation, while barchans dunes indicate a typically one-directional wind regime (Tsoar, 1984). However, we find that there are combinations of barchan and linear dunes in both the Qaidam Basin and on Mars (Fig. 9, 10). Three mechanisms causing asymmetry of barchans and forming linear dunes have been identified: bi-directional winds, dune collision, and topography (Bourke, 2010). However, our field survey and image interpretation argue for additional causes, such as an obstacle at the leading edge of the dune could cause the formation of a linear dune (e.g., yadangs, Fig. 10A), stabilization from the bottom due to a wet base in and surrounding the base of the dune (Fig. 10B), and stabilization atthe top of the dune due to a salt crust along the dune's surface (Fig. 10C, D). Thus, asymmetry and linear dunes on Mars could be formed through many additional mechanisms and this could have significant implications for understanding martian environments.

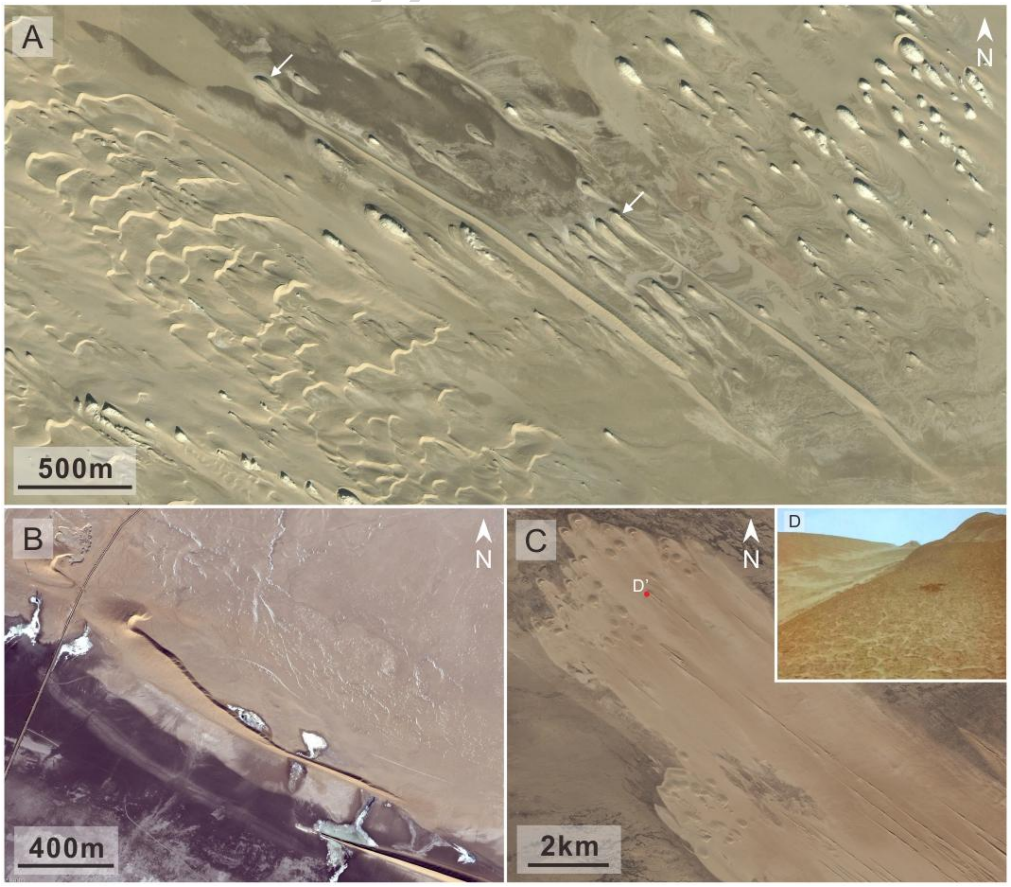

Figure 9. Combinations of barchans, linear dunes, and yardangs in the Qaidam Basin. (A) The combination of a barchan dune field (lower left) and yardangs (upper right). Note that the shape and orientation of yardangs and barchans all indicate that the wind direction is from the upper left to lower right. Here, linear dunes formed behind some yardangs, as indicated by white arrows. (B) A linear dune co-exists with a barchan dune (asymmetric dune) due to a wet base. (C) In the combination of barchans and linear dunes in the Qaidam Basin, in which case the surfaces of the dunes are covered by a salt crust (D, photo is courtesy of Prof. Dong Zhibao).

At Chasma Boreale, the polar region of Mars, there are also combinations of barchans and linear dunes(Dial Jr and Dohm, 1994) (Fig. 10). Both of the dark barchans dunes and white stripes (made of dry ice) indicate that the wind direction is from northeast to southwest. Most the barchans are aligned, and some of them are heads of linear dunes (Fig. 10A). As high-resolution images do not show salt crust on the dune surfaces (Fig. 10C), this combination could be formed by a wet base in the area, similar to that seen in Figure 9B, or more likely the linear dunes formed after the barchan dunes and the head barchans played a role in obstructing, in a manner similar to yardangs at the Qaindam Basin (Fig. 9A).

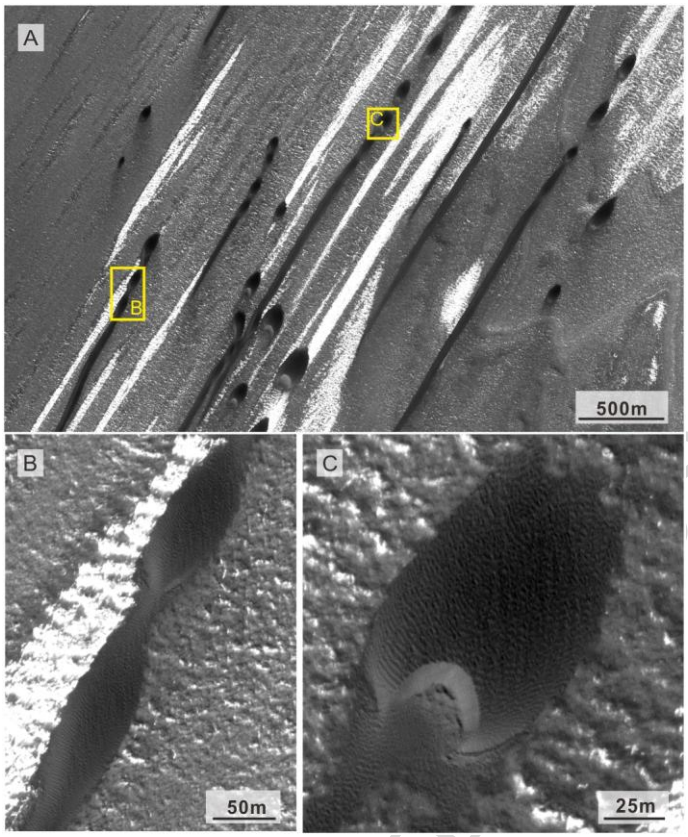

Figure 10. Portion of Moc image E0100104 showing a combination of linear and barchan dunes at Chasma Boreale on Mars (83.9N, 535 40.5W) with enlargements of the image detailing (B) a linear dune and (c) a barchan dune.

Yardangs are relatively less studied aeolian landforms in comparison to dunes. In this context, the well-observable yardangs in the Qaidam Basin may provide insights into similar features on Mars. Yardangs could have formed through the erosion of sedimentary rocks by both water and wind. The contributions of the two major forces can be distinguished by yardang distributions, morphologies, and environments. Mesa yardangs are the initial form of yardangs. They are interpreted to usually have formed through water erosion of sedimentary deposits. In addition, subsequent winds directed through gaps in the mesa yardang, and gap enlargement over time, leads to segment mesa yardangs (i.e., small individual yardangs). The ridges of these individual yardang form parallel to and taper in the direction of prevailing winds. The geometries of yardangs reveal the prevailing wind pattern during their developments (Kapp et al., 2011). Northwesterly winds enter the Qaidam Basin through topographic lows in the Altyn Tagh Range

along its northwestern margin (Fig. 2A, (Halimov and Fezer, 1989)). The wind direction turns NW-SE to nearly W-E, which consists with the change of >5000-m-high basin-bounding mountain ranges. (Kapp et al., 2011). Rainfall, desiccation cracking, weathering, and mass movements also contribute to the formation of yardangs. These basic observations could shed light on the main geological processes shaping yardangs on Mars (Fig. 4). Yardangs on Mars are mainly distributed in the equatorial region, and they are usually explained as the product of time-integrated, changing wind regimes over long timescales. Recent exploration by the Curiosity rover at the Gale crater (Fig. 4D') provides a close view of the yardangs in the crater. Detailed comparative study of the difference and similarity of yardangs in the Qaidam Basin and on Mars will provide new analogues and lead to a better understanding of their formation in the past and today.

6.2 Gullies, fluvial valleys, and alluvial fans

On Mars, thousands of gullies have been identified in high-resolution images (Harrison et al., 2015; Malin and Edgett, 2000). They are found on dunes, valley or crater walls, and hillsides (Dickson et al., 2007; Diniega et al., 2010; Hobbs et al., 2015; Johnsson et al., 2014). Gullies on Mars and in the Qaidam Basin have similar morphologic features. For example, alcoves can be observed in the head part of gullies, and the width of the gullies will decrease with elevation on both the Earth (Fig. 6A) and Mars (Fig. 6B). Most of gullies on Mars are considered as indications of recent geologic activities (Malin and Edgett, 2000), but the origin of them is still controversial, including debris flows with groundwater, liquid CO_2 flows, melting of snow or ice, mass wasting, among others (Christensen, 2003; Harrison et al., 2015; Musselwhite et al., 2001). A comparative study of the morphology and geologic background of gullies on Mars and in the Qaidam Basin could be an effective way to constrain the origin of martian gullies.

Valleys on Mars are mainly distributed in the southern highlands, and most of them are considered to be incised by liquid water (Carr, 1995; Fassett and Head, 2008a; Gulick, 2001; Howard et al., 2005). Some valley network patterns on Mars are analogues to those in the Qaidam Basin, though the former are much larger in scale (Fig. 8). Many factors should be considered in valley formation: source of water, bedrock properties, original landforms, local climate, later

modification processes, and so on. For example, groundwater sapping usually forms narrow valleys in the southern highland, while cataclysmic release of groundwater or meltwater can lead to the formation of large valley systems or even outflow channels (Gulick, 2001; Komatsu and Baker, 2007). As another example, a V-shaped valley may represent rapid downcutting by runoff along a steep gradient, with little subsequent modification. On the contrary, a valley formed in a flat inter-crater plain, with relatively longer term runoff resulting in a U-shaped cross-section (Gulick, 2001; Irwin et al., 2008). Bedrock property may also be a major factor. As we observed with the two valley types of in the Qaidam Basin (Fig. 8), the morphological difference mainly results from different bedrock types. Granitic bedrocks are much harder to erode compared with sand-mudstone. Therefore, with the same precipitation level and slope angle, water in a granitic bedrock tends to form wide but relatively shallow valleys (Fig. 8A), while water in a sand-mudstone mountain deeply incises the surface and forms narrow and deep valleys (Fig. 8B). On Mars, bedrock property could also be different due to a specific and distinct origin, e.g. sedimentary, lava flows, pyroclastic rocks (Carr, 2007; Huang and Xiao, 2014; Xiao et al., 2012; Xiao and Wang, 2009), as well as possible ancient felsic basement, which could include granite (2014; 2013; 2015; Dohm et al., 2009). Thus, a comprehensive study of the origin of different types of valleys is required.

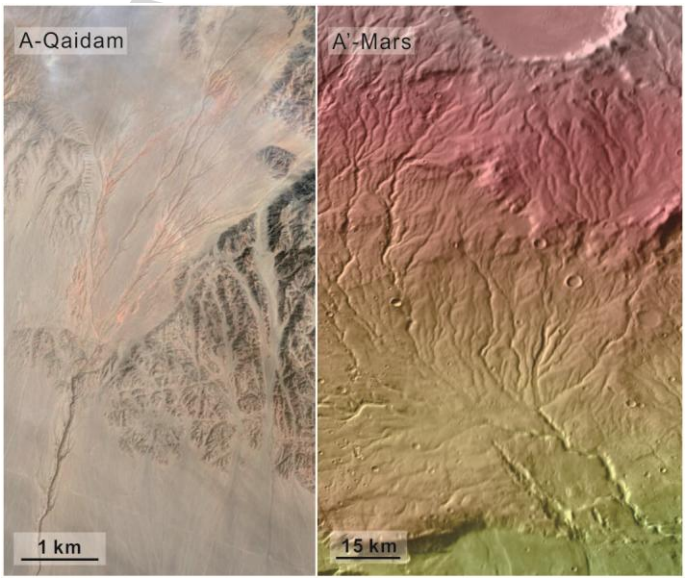

Figure 11. Valley networks in the Qaidam Basin (A, central coordinates: 92.59°E, 38.84°N; image credit: Google Earth) and on Mars (B, central coordinates: 267.33°E, -41.96°N; The background image is THEMIS daytime IR data overlaid by MOLA colorized topographic map).

Alluvial fans and fan deltas have been widely identified on Mars (Achille and Hynek, 2010; Moore and Howard, 2005). They are usually distributed in craters and in Valles Marineris, and are important evidence for the existence of surface water on early Mars (Baker, 2001; Moore and Howard, 2005). The fan morphology has been considered as an indicator of the climate and environment. For example, Cabrol and Grin (2001) proposed that apron-shaped alluvial fan/deltas on Mars indicate a relatively arid period, while an elongate shape indicates a high-discharge period. However, examples from the Qaidam Basin indicate that the link between fan morphology and the climate could be more complicated. The alluvial fans in Figure 11 are formed under the same climate conditions, and their morphologic types are dominated by the velocity of the water from the valleys. Specifically, as the main stream of the valley in Figure 11A is much wider than that in Figure 11B, the velocity of water in it should be lower with the same discharge. This leads to the formation of an apron-shaped alluvial fan at the end of the valley rather than an elongate fan. Therefore, further research is needed to determine the factors affecting the morphology of martian alluvial fans, especially the relationship between fan morphology and the appropriate environmental conditions.

6.3 Desiccation polygons

Polygons are widespread on both Earth and Mars. They are known to have several formation mechanisms, including volcanic, tectonic, desiccation, and thermal contraction (El Maarry et al., 2010; Lachenbruch, 1962; Lucchitta, 1983; Mangold, 2005; Mutch et al., 1976; Pechmann, 1980). Polygonal crack patterns resulting from volcanic processes can often be formed in basaltic columns, while tectonic processes usually produce kilometer-sized polygons such as the polygons located in the northern plains of Mars (McGill and Hills, 1992; Pechmann, 1980). Due to local climatic conditions, the desiccation and thermal contraction would most likely be the main potential reason for the formation of PSSs that occur within the Qaidam Basin. In the past,

lakes and water-rich sediments occupied the basin, which would have experienced an active hydrological cycle indicated by widespread distribution of playas (Chen and Bowler, 1986; Komatsu et al., 2007). The kind of observable polygon/crack morphology tends to form on surfaces made by salt crust or mud which entraps aeolian sands and authigenic evaporitic minerals (Komatsu et al., 2007).

Polygons on Mars vary in size from 2 to 3 m, and all the way up to 10 km in diameter (El Maarry et al., 2010). With very few exceptions, small-scale polygonal terrain occurs at middle to high latitudes of the northern and southern hemispheres in Hesperian-age (~3.7-3.1 G.yr) geologic units (Seibert and Kargel, 2001). Furthermore, middle to large-sized (>10 m) PSSs, which occur mainly in impact crater floors (Fig. 5C'), and appear to be mainly located in high latitudes on Mars (30^{o}–75^{o}), are considered to be markers of dried-up bodies of water inside impact crater basins (El Maarry et al., 2010). This is consistent with the distribution of valley network-fed, open-basin lakes on Mars (Fassett and Head, 2008a). Many indicators of paleolakes, including channels, lacustrine deltas, terraces, shorelines, evaporates, and layered sedimentary deposits, have been identified in impact craters (basins) on Mars (Cabrol and Grin, 1999). In addition, possible paleo-shorelines in the northern plains (Parker et al., 1989) and crater lakes (Cabrol and Grin, 1999; Malin and Edgett, 2003; Ori et al., 2000) have been defined by remote sensing surveys. El Maarry et al. (2010) mapped other geomorphologic features (e.g., mounds, layered sediments, deltas, putative shorelines) related to lake bodies associated with crater floor polygons which corroborates that the impact craters once contained lakes.

Many ancient saline lakes and associated playas have been suggested to have formed on Mars based on the occurrence of polygons and evaporate minerals (El Maarry et al., 2013). This is strongly supported by the existence of halite and chlorite content, which has been detected in the martian polygonal terrain indicated by Figure 5B' (El Maarry et al., 2010; Osterloo et al., 2008). As observed in the Qaidam Basin, most polygons have raised rims; large-sized polygons especially, have remarkable raised rims and no cracks (Fig. 5D). Interestingly, we also find raised-rim PSSs on the Roddy Crater floor on Mars (Fig. 5D'). This is different from the polygons

that occur in the high-latitude regions, where permafrost or frost layers formed cracks and gaps defining polygons. The morphology of the prominent rim pattern is often observed in halite surfaces (Komatsu et al., 2007) in playas elsewhere. A possible formation mechanism of the raised rim can be summarized as the following four stages (Komatsu et al., 2007; Ma et al., 2011; Schubel and Lowenstein, 1997): (1) the deposition of salts occurs in the subsurface; (2) the evaporation of water contained in sediment pores; (3) ascent of brine into the drying layer; and (4) successive halite crystals grow in brine-filled salt layers as cement and trigger inflation of the polygonal rim. Therefore, the occurrence of the prominent rim-defined polygons is probably a good indicator of the presence of playas made of salts, similar to that observed in the Qaidam Basin.

6.4 Playas and evaporate sediments

A series of evaporitic sediments, including carbonates, sulfates, and chlorides, the formation of which is associated with hydrological process (Osterloo et al., 2008; Zheng et al., 2013) have been detected and identified by multiple instruments (THEMIS, OMEGA and CRISM) on board previous Mars missions (Arvidson et al., 2005; Ehlmann et al., 2008; Michalski and Niles, 2010; Morris et al., 2010; Osterloo et al., 2008). This implies that oceans or lakes have existed stably in Mars history, and have changed to dry lake or playa environments, owing to the decrease or evaporation of water, and that they eventually desiccated completely (Achille and Hynek, 2010). This is also suggested by the studies on martion paleolakes (Fassett and Head, 2008b; 2015; Goudge et al., 2012). Thus, identification and research of playas on Mars has great significance for studying its ancient hydrologic history.

Playa environments are characterized by an active hydrological cycle, water-generated landforms, and evaporitic sediments, which primarily occur in dry regions of the Earth (Komatsu et al., 2007). Many salt-rich lacustrine playas on Earth have been taken as terrestrial analogues, such as Chott el Jerid of North Africa, Lucerne playa and Death Valley of USA, the Dalangtan playa of China. among others (Baldridge et al., 2004; El Maarry et al., 2013; Komatsu et al., 2007; Kong et al., 2014). The depositional and weathering processes of hydrated sulfates based on the natural environment of the Dalangtan playa, which is similar to Mars, and the widespread kieserite

on Mars have formed through weathering of hydrated Mg-sulfates under current Mars conditions (Kong et al., 2014). As discussed above, the Qaidam Basin, a typical inland plateau basin, is one of the most arid regions on Earth. With the playa being the dominant style today, multiple lacustrine sedimentary centers occur inside the basin, and the Dalangtan playa is one of them. Sulfates and chlorides are the main composition of salts deposited in the Qaidam Basin. This is similar to the types of sedimentary salt found on Mars (Gendrin et al., 2005; Osterloo et al., 2010).

6.5 Habitability

The search for traces of life is one of the principal objectives of Mars exploration. Central to this objective is the concept of habitability, the set of conditions that allows the appearance of life and successful establishment of microorganisms in any one location. It would be preferable to search for biosignatures at a location where they could have been concentrated, as in hydrothermal, lacustrine, or paleosol sedimentary environments (Fairén et al., 2010). To ensure better chances of preservation, the geological units should have undergone limited diagenesis, and the rocks should have not experienced prolonged contact with the martian surface and its atmosphere, where oxidizing conditions and radiation would have destroyed much of the organic components.

Terrestrial analogue sites represent vital tools in our continued study of the Red Planet. Generally, extremely aridity, high radiation, and oxidizing soils characterize modern-day Mars, while acid–saline waters would have presented their own challenges during the planet's wetter past (Marlow et al., 2011). Previous studies have shown the taxonomic diversity of microbial populations and preserved signatures of Mars-analogue environments that approximate these two Martion conditions of a wetter past and much more arid present (Fernández-Remolar et al., 2013; Fernández-Remolar et al., 2005; Yang et al., 2015). The most sought-after arid organic host analogue location is the Atacama Desert in northern Chile, where the offshore Humboldt Current, the Pacific anticyclone, and the Andes Mountains conspire to maintain hyper-arid conditions. Organic content is very low throughout the Atacama, and is dominated by halophilic and halotolerant microbes (Stivaletta et al., 2011; Yang et al., 2015). The acid–saline lakes of the Yilgarn Craton of Western Australia are sedimentologically and mineralogically similar to depositional environments on Mars, as they boast salinities up to 28% total dissolved solids and

pHs as low as 1.5 (Benison and Bowen, 2006). Bacteria and archaea have been identified in the acid–saline lakes of Western Australia (Hong et al., 2006), and acidophilic microbial colonies are readily visible (Bowen et al., 2008). However, most of the above analogue sites only represent parts of the present Mars-like geomorphologic and possible environmentalconditions of formation. To trace the history of these geological features and environmental changes, we need a site where there are not only dry desert landforms, but also partially preserved wet saline lake records.

Playas in the Qaidam Basin are covered by evaporates. Distributions of the salt minerals, clays, and other minerals in the subsurface have recorded climate change in its history (Ma et al., 2011; QIN et al., 2012). Sediments of the Dalangtan playa are characterized by high concentration of salts, low organic carbon enrichment, and slightly alkaline condition. Major species among the isolated microbes, were *Bacillus*, which were capable of producing spores to help resist harsh environments (Colao et al., 2004). Besides *Bacillus*, moderately halophilic bacteria form a relatively large percentage of the population in this area. More facts need to be compiled in further studies in order to get more details about this microbial eco-system.

6.6 Potential mission simulation and test site

Several terrestrial analogue sites have been established worldwide (Farr, 2004). They are chosen for their locations, which simulates a specific aspect of conditions that people could experience during a future mission to Mars: e.g., high altitudes can simulate low pressure of the martian atmosphere (Chilean Altiplano, (Garcia-Castellanos, 2007)); high latitudes can provide solar radiation similar to the martian surface (Flashline Mars Arctic Research Station, (Bamsey et al., 2009)); hot and cold deserts such as the Atacama as an example of the former (Romig et al., 2007) and the Antarctic Dry Valleys an example of the latter (Head and Marchant, 2014; Marchant and Head, 2007); and acid lakes (Gneiss Lake & Rio Tinto, (Marlow et al., 2011)) are good candidates for astrobiology studies; volcanic regions (Hawaii Space Exploration Analog and Simulation, (Binsted, 2015)) can provide similar geologic characteristics of the martian surface.

The Qaidam Basin is a unique site compared to other Mars analogues based on the observations presented above. These include: extensive aeolian geologic features, a variety of

evaporate sediments, saline lakes with different geochemistry, playas, and bio-signatures in extreme environments. It is remote but accessible, and can serve as a good analogue site for future Chinese and international surface robotic/human missions destined for Mars. For a robotic mission, several scientific experiments can be carried out:

(1) In-situ mineralogy and elemental analysis. Surface materials in the Qaidam Basin vary in mineralogy and elements as described above; in-situ mineralogy and elemental measurements on the surface could provide "ground truth" for orbital remote sensing data. Several existing scientific instruments could be tested and field-proven in the Qaidam Basin. For instance, the Advanced Space borne Thermal Emission and Reflection Radiometer (ASTER; http://asterweb.jpl.nasa.gov/) instrument on the Earth Observing System platform Terra are similar to THEMIS. A field infrared spectrometer can provide mineralogical information similar to data of the Mini-TES (Christensen et al., 2004a) onboard Spirit and Opportunity. In addition, other mineralogical and elemental experiments (e.g. (Edwards et al., 2007; Wang and Zheng, 2009), testing the Near-Infrared Spectrometer (Lynch et al., 2015), and an X-ray diffraction/fluorescence imager (Sarrazin et al., 2005), for example, can be performed in the Qaidam Basin.

(2) High-resolution geomorphology and topography. Diverse geologic features (e.g. dunes, polygons, yardangs, valleys, and Gullies) have been identified in the Qaidam Basin, which are similar to those on Mars. However, the detailed geomorphology and topography information is limited due to the spatial resolution of terrestrial orbital data. Therefore, imaging data from Unmanned Aerial Vehicles (UAVs) and remotely-controlled rovers would be important for detailed geomorphological and sedimentological studies of these geological features. With appropriate designs (Tonkin et al., 2014) of the imaging procedure and algorithm of Digital Elevation Model (DEM), high resolution topographic information (~30 cm/pix) can be derived.

(3) Robotic drilling. Life or bio-signature are difficult to retain or be preserved on the surface of the Qaidam Basin, similar to the harsh surface environment on Mars. However, life and possible biosignature have been found several centimeters beneath the surface of dry salt lake deposits as described above. In addition, although the surface of both the Qaidam Basin and Mars

are extremely dry, liquid water has been identified beneath the surface (Martín-Torres et al., 2015). A robotic drilling project could gain direct access to liquid water, and search for life and bio-signature in the subsurface material. A core sample could be examined by remote sensing instruments including a panoramic context imager, microscopic imager, and a visible-near infrared hyperspectral imager.

（4） Geophysical measurements. It is very important to have insights into internal structure of various geological features and complex lake deposits. In situ penetrating radars (Xiao et al., 2015) and seismic instruments (Panning et al., 2015) are successfully applied in deciphering subsurface structure of geologic features on the Moon. Other geophysical measurements (e.g., gravity, electric, and magnetic) could also be carried out in the field of the Qaidam Basin to provide essential information.

Besides the scientific measurements by a robotic mission mentioned above, a simulated human mission can study the effectiveness of new designs for space suits, robots, rovers, surface networking and communications, exploration information systems and computing, habitats, and other equipment, and gain experience in the use of new technologies designed to make planetary exploration safer, easier, and more efficient.

7 Concluding remarks

(1) The Qaidam Basin is the highest and one of the largest and driest deserts on Earth. It is located at a dry, cold, and high UV environment, similar to the surface of Mars.

(2) A variety of aeolian landforms is widely distributed in the desert regions of the Qaidam Basin. Most geomorphological types of dunes and yardang have their counterparts on Mars. Detailed study of the origins of dunes and yardangs could provide clues to the understanding of how wind operated and/or is operating, and how the source and sink relationships work on Mars.

(3) Precipitation in the Qaidam Basin is very low; and the gullies, valleys, and fluvial fans are distributed along the surrounding hillsides. Small water-driven mass transportation, mass wasting, and deposition formed distinct fluvial landforms, similar to those on Mars.

(4) Saline lakes and playas represent different stages of lake evolution, Which provides unique examples to study how lakes changed from fresh to hypersaline ones, and finally to playas. As variable evaporate mineral assemblages have been identified in playas in the Qaidam Basin, the origin of their counterparts on Mars could be inferred.

(5) The microbial system in saline lakes and playas exist in different degrees, although there is no visible life signature in most playas and hypersaline lakes. Field-based investigations have shown that halophiles were the most important fraction in the hypersaline sediments of arid environments, which includes the taxa of the three domains of life: archaea, bacteria, and eucarya. It is suggested that playas on Mars are candidate sites for searching for martian life.

(6) The variety of exogenic and endogenic geomorphic types, sedimentary rocks, evaporite mineral assemblages, and Mars-like extreme environment collectively makes the Qaidam Basin an excellent new martian analogue site on Earth, for both Mars-driven scientific research and future mission testing.

Acknowledgements

We thank Jim Head and James Dohm for their helpful review comments. This study was supported by Nature Science Foundation of China (Grant No. 41373066), Specialized Research Fund for the Doctoral Program of Higher Education (Grant No. 20130145130001) and the Science and Technology Development Fund (FDCT) of Macau (Grant No. 107/2014/A3 and 039/2013/A2). We thank the State Key Laboratory of Biogeology and Environmental Geology (China University of Geosciences, Wuhan, China) for providing microorganic and geochemical experiment support. We thank Prof. Hongcheng Jiang for providing the mineralization and pH data listed in Table 2. Dr. David Fernández-Remolar and Dr. Zhongping Lai are thanked for constructive discussion and improvement of the manuscript. Mr. Le Qiao, Mrs. Zuoqing Xue, Mrs. Xiaoqian Liu, Mr. Limin Zhao, Mr. Yu Wei, Mr. Fan Zou and Mr. Bo Wang are thanked for fieldwork assistance.

References

Achille, G.D. and Hynek, B.M., 2010. Ancient ocean on Mars supported by global distribution of deltas and valleys. Nature Geoscience, 3(7): 459-463.

Arvidson, R. et al., 2005. Spectral reflectance and morphologic correlations in eastern Terra Meridiani, Mars. Science, 307(5715): 1591-1594.

Baker, V.R., 2001. Water and the Martian landscape. Nature, 412(6843): 228-236.

Baker, V.R. and Nummedal, D., 1978. The channeled scabland: a guide to the geomorphology of the Columbia Basin, Washington: prepared for the Comparative Planetary Geology Field Conference held in the Columbia Basin, June 5-8, 1978. National Aeronautics and Space Administration.

Baldridge, A.M., Farmer, J.D. and Moersch, J.E., 2004. Mars remote‐sensing analog studies in the Badwater Basin, Death Valley, California. Journal of Geophysical Research: Planets, 109(E12).

Bamsey, M. et al., 2009. Four-month Moon and Mars crew water utilization study conducted at the Flashline Mars Arctic Research Station, Devon Island, Nunavut. Advances in Space Research, 43(8): 1256-1274.

Bao, F. and Dong, Z., 2014. Grain Size Characteristics of Sediments from Typical Sand Dunes in Chaerhan Salt Lake. Bulletin of Soil and Water Conservation, 34(6).

Bao, F. and Dong, Z., 2015. Mineral composition and origin of surface sediment in the desert of the Qaidam Basin. Journal of Northwest University(Natural Science Edition)

Bell, J., 2008. The Martian Surface: Composition, Mineralogy and Physical Properties. Cambridge University Press.

Benison, K.C. and Bowen, B.B., 2006. Acid saline lake systems give clues about past environments and the search for life on Mars. Icarus, 183(1): 225-229.

Bibring, J.-P. et al., 2005. Mars Surface Diversity as Revealed by the OMEGA/Mars Express Observations. Science, 307(5715): 1576-1581.

Binsted, K., 2015. Hawai'i Space Exploration Analog and Simulation.

Bocco, G., 1991. Gully erosion: processes and models. Progress in physical geography, 15(4): 392-406.

Bourke, M. and Zimbelman, J., 2001. The Australian paleoflood model for unconfined fluvial deposition on Mars, Lunar and Planetary Science Conference, pp. 1679.

Bourke, M.C., 2010. Barchan dune asymmetry: Observations from Mars and Earth. Icarus, 205(1): 183-197.

Bourke, M.C. and Goudie, A.S., 2009. Varieties of barchan form in the Namib Desert and on Mars. Aeolian Research, 1(1): 45-54.

Bowen, B.B., Benison, K., Oboh-Ikuenobe, F., Story, S. and Mormile, M., 2008. Active hematite concretion formation in modern acid saline lake sediments, Lake Brown, Western Australia. Earth and Planetary Science Letters, 268(1): 52-63.

Bridges, N.T. et al., 2012. Planet-wide sand motion on Mars. Geology, 40(1): 31-34.

Cabrol, N. and Grin, E., 2001. The Evolution of Lacustrine Environments on Mars: Is Mars Only Hydrologically Dormant? Icarus, 149(2): 291-328.

Cabrol, N.A. and Grin, E.A., 1999. Distribution, classification, and ages of Martian impact crater lakes. Icarus, 142(1): 160-172.

Cabrol, N.A. et al., 2007. Life in the Atacama: Searching for life with rovers (science overview).

Journal of Geophysical Research: Biogeosciences, 112(G4).

Cardinale, M., Komatsu, G., Silvestro, S. and Tirsch, D., 2012. The influence of local topography for wind direction on Mars: two examples of dune fields in crater basins. Earth Surface Processes and Landforms, 37(13): 1437-1443.

Cardinale, M. et al., 2016. Present-day aeolian activity in Herschel Crater, Mars. Icarus, 265: 139-148.

Carr, M.H., 1995. The Martian drainage system and the origin of valley networks and fretted channels. Journal of Geophysical Research: Planets (1991–2012), 100(E4): 7479-7507.

Carr, M.H., 2007. The surface of Mars, 6. Cambridge University Press.

Chan, M.A., Nicoll, K., Ormö, J., Okubo, C. and Komatsu, G., 2011. Utah's geologic and geomorphic analogs to Mars—An overview for planetary exploration. Geological Society of America Special Papers, 483: 349-375.

Chan, M.A., Jewell, P.W., Parker, T.J., Ormö, J., Okubo, C.H., Komatsu, G., 2016. Pleistocene Lake Bonneville as an analog for extraterrestrial lakes and oceans. In: Oviatt, C.G., Shroder, J.F. (eds.), Lake Bonneville: A Scientific Update. Developments in Earth Surface Processes v. 20, Elsevier, Amsterdam, pp. 570–597, doi: 10.1016/B978-0-444-63590-7.00021-4.Chang, H. et al., 2015. Magnetostratigraphy of Cenozoic deposits in the western Qaidam Basin and its implication for the surface uplift of the northeastern margin of the Tibetan Plateau. Earth and Planetary Science Letters, 430: 271-283.

Chapman, M., 2007. The Geology of Mars: Evidence from Earth-Based Analogs. Cambridge University Press.

Chen, K. and Bowler, J., 1986. Late Pleistocene evolution of salt lakes in the Qaidam basin, Qinghai province, China. Palaeogeography, Palaeoclimatology, Palaeoecology, 54(1): 87-104.

Christensen, P. et al., 2004a. Mineralogy at Meridiani Planum from the Mini-TES experiment on the Opportunity Rover. Science, 306(5702): 1733-1739.

Christensen, P.R., 2003. Formation of recent Martian gullies through melting of extensive water-rich snow deposits. Nature, 422(6927): 45-48.

Christensen, P.R. et al., 2001. Mars Global Surveyor Thermal Emission Spectrometer experiment: Investigation description and surface science results. Journal of Geophysical Research-Planets, 106(E10): 23823-23871.

Christensen, P.R. et al., 2004b. The Thermal Emission Imaging System (THEMIS) for the Mars 2001 Odyssey Mission. Space Science Reviews, 110(1-2): 85-130.

Christiansen, F., 1963. Polygonal fracture and fold systems in the salt crust, Great Salt Lake Desert, Utah. Science, 139(3555): 607-609.

Clarke, J.D. et al., 2006. A multi-goal Mars analogue expedition (expedition two) to the Arkaroola region, Australia. Mars Analog Research. Science and Technology Series, 111: 3-15.

Colao, F. et al., 2004. Investigation of LIBS feasibility for in situ planetary exploration: an analysis on Martian rock analogues. Planetary and Space Science, 52(1): 117-123.

Dial Jr, A. and Dohm, J.M., 1994. Geologic map of science study area 4, Chasma Boreale region of Mars.

Dickson, J.L., Head, J.W. and Kreslavsky, M., 2007. Martian gullies in the southern mid-latitudes of Mars: Evidence for climate-controlled formation of young fluvial features based upon local and global topography. Icarus, 188(2): 315-323.

Diniega, S., Byrne, S., Bridges, N.T., Dundas, C.M. and McEwen, A.S., 2010. Seasonality of present-day Martian dune-gully activity. Geology, 38(11): 1047-1050.

Dohm, J., Maruyama, S., Miyamoto, H., Viviano-Beck, C. and Anderson, R., 2014. Accretionary Complexes: Recorders of Plate Tectonism and Environmental Conditions Through Time on Earth and Possibly Those Early Noachian (Hadean-equivalent) in Age on Mars, AGU Fall Meeting Abstracts, pp. 07.

Dohm, J. et al., 2013. Mars evolution, Nova Science Publishers, Inc.

Dohm, J. et al., 2011. An inventory of potentially habitable environments on Mars: Geological and biological perspectives. Geological Society of America Special Papers, 483: 317-347.

Dohm, J. et al., 2015. The Mars plate-tectonic-basement hypothesis, Lunar and Planetary Science Conference, pp. 1741.

Dohm, J.M. et al., 2009. Claritas rise, Mars: Pre-Tharsis magmatism? Journal of volcanology and geothermal research, 185(1): 139-156.

Dohm, J.M. et al., 2004. The Northwestern Slope Valleys (NSVs) region, Mars: A prime candidate site for the future exploration of Mars. Planetary and Space Science, 52(1): 189-198.

Dyall-Smith, M., 2009. The Halohandbook: Protocols for Halobacterial Genetics. 2009 http://www. haloarchaea. com/resources/handbook. Halohandbook_2009_v7.

Edwards, H.G. et al., 2007. The Rio Tinto Mars analogue site: an extremophilic Raman spectroscopic study. Spectrochimica Acta Part A: Molecular and Biomolecular Spectroscopy, 68(4): 1133-1137.

Edwin D, M., 1979. A study of global sand seas.

Ehlmann, B.L. et al., 2008. Orbital identification of carbonate-bearing rocks on Mars. Science, 322(5909): 1828-1832.

El Maarry, M. et al., 2010. Crater floor polygons: Desiccation patterns of ancient lakes on Mars? Journal of Geophysical Research: Planets (1991–2012), 115(E10).

El Maarry, M., Pommerol, A. and Thomas, N., 2013. Analysis of polygonal cracking patterns in chloride-bearing terrains on Mars: Indicators of ancient playa settings. Journal of Geophysical Research: Planets, 118(11): 2263-2278.

El Maarry, M.R., Kodikara, J., Wijessoriya, S., Markiewicz, W.J. and Thomas, N., 2012. Desiccation mechanism for formation of giant polygons on Earth and intermediate-sized polygons on Mars: Results from a pre-fracture model. Earth and Planetary Science Letters, 323: 19-26.

Essefi, E., Komatsu, G., Fairén, A.G., Chan, M.A. and Yaich, C., 2014a. Groundwater influence on the aeolian sequence stratigraphy of the Mechertate–Chrita–Sidi El Hani system, Tunisian Sahel: Analogies to the wet–dry aeolian sequence stratigraphy at Meridiani Planum, Terby crater, and Gale crater, Mars. Planetary and Space Science, 95: 56-78.

Essefi, E., Komatsu, G., Fairén, A.G., Chan, M.A. and Yaich, C., 2014b. Models of formation and activity of spring mounds in the Mechertate-Chrita-Sidi El Hani System, Eastern Tunisia: implications for the habitability of Mars. Life, 4(3): 386-432.

Fairén, A.G. et al., 2010. Astrobiology through the ages of Mars: the study of terrestrial analogues to understand the habitability of Mars. Astrobiology, 10(8): 821-843.

Fan, Q.S., Ma, H.Z., Tan, H.B., Li, T.W. and Xu, J.X., 2007. Hydrochemical Characteristics of Brines and Potassium-Prospecting Researches in Western Qaidam Basin. Acta Geoscientica Sinica.

Farr, T.G., 2004. Terrestrial analogs to Mars: The NRC community decadal report. Planet Space Sci,

52(1): 3-10.

Fassett, C.I. and Head, J.W., 2008a. The timing of martian valley network activity: Constraints from buffered crater counting. Icarus, 195(1): 61-89.

Fassett, C.I. and Head, J.W., 2008b. Valley network-fed, open-basin lakes on Mars: Distribution and implications for Noachian surface and subsurface hydrology. Icarus, 198(1): 37-56.

Fernández-Remolar, D.C. et al., 2013. Molecular preservation in halite - and perchlorate - rich hypersaline subsurface deposits in the Salar Grande basin (Atacama Desert, Chile): Implications for the search for molecular biomarkers on Mars. Journal of Geophysical Research: Biogeosciences.

Fernández-Remolar, D.C., Morris, R.V., Gruener, J.E., Amils, R. and Knoll, A.H., 2005. The Rio Tinto Basin, Spain: mineralogy, sedimentary geobiology, and implications for interpretation of outcrop rocks at Meridiani Planum, Mars. Earth and Planetary Science Letters, 240(1): 149-167.

Fernández-Remolar, D.C. et al., 2008. Underground habitats in the Río Tinto basin: a model for subsurface life habitats on Mars. Astrobiology, 8(5): 1023-1047.

Foing, B. et al., 2011. Field astrobiology research in Moon–Mars analogue environments: instruments and methods. International Journal of Astrobiology, 10(03): 141-160.

Fryberger, S.G. and Dean, G., 1979. Dune forms and wind regime. A study of global sand seas, 1052: 137-169.

Fu, Y., Xiao, J. S., Xiao, R. X., Zhang, J., Liu, B. K., Su, W. J., Li, F. and Feng, S. Q., 2008. Impact of Climate Change on Water Resources in the Qaidam Basin-A Case Study in the Keluke Lake Basin. Journal of Glaciology and Geocryology, 30(6): 998-1006.

Garcia-Castellanos, D., 2007. The role of climate during high plateau formation. Insights from numerical experiments. Earth and Planetary Science Letters, 257(3–4): 372-390.

Gendrin, A. et al., 2005. Sulfates in Martian layered terrains: the OMEGA/Mars Express view. Science, 307(5715): 1587-1591.

Goudge, T.A., Aureli, K.L., Head, J.W., Fassett, C.I. and Mustard, J.F., 2015. Classification and analysis of candidate impact crater-hosted closed-basin lakes on Mars. Icarus, 260: 346-367.

Goudge, T.A., Head, J.W., Mustard, J.F. and Fassett, C.I., 2012. An analysis of open-basin lake deposits on Mars: Evidence for the nature of associated lacustrine deposits and post-lacustrine modification processes. Icarus, 219(1): 211-229.

Greeley, R. and Fagents, S.A., 2001. Icelandic pseudocraters as analogs to some volcanic cones on Mars. Journal of geophysical research, 106(20): 527-20.

Greeley, R., White, B.R., Pollack, J.B., Iversen, J.D. and Leach, R.N., 1981. Dust storms on Mars: Considerations and simulations. Geological Society of America Special Papers, 186: 101-122.

Grotzinger, J.P. et al., 2014. A Habitable Fluvio-Lacustrine Environment at Yellowknife Bay, Gale Crater, Mars. Science, 343(6169).

Gulick, V.C., 2001. Origin of the valley networks on Mars: A hydrological perspective. Geomorphology, 37(3): 241-268.

Halimov, M. and Fezer, F., 1989. 8 yardang types in Central-Asia. Zeitschrift fur Geomorphologie, 33(2): 205-217.

Harrison, T.N., Osinski, G.R., Tornabene, L.L. and Jones, E., 2015. Global documentation of gullies with the Mars Reconnaissance Orbiter Context Camera and implications for their formation.

Icarus, 252: 236-254.

Hauber, E. et al., 2011. Periglacial landscapes on Svalbard: Terrestrial analogs for cold-climate landforms on Mars. Geological Society of America Special Papers, 483: 177-201.

Hayward, R.K. et al., 2007. Mars Global Digital Dune Database and initial science results. Journal of Geophysical Research, 112(E11).

Head, J.W. and Marchant, D.R., 2014. The climate history of early Mars: insights from the Antarctic McMurdo Dry Valleys hydrologic system. Antarctic Science, 26(06): 774-800.

Hesp, P., Hyde, R., Hesp, V. and Zhengyu, Q., 1989. Longitudinal dunes can move sideways. Earth Surface Processes and Landforms, 14(5): 447-451.

Hobbs, S.W., Paull, D.J. and Clarke, J.D.A., 2015. Analysis of regional gullies within Noachis Terra, Mars: A complex relationship between slope, surface material and aspect. Icarus, 250: 308-331.

Hong, B.-y. et al., 2006. Microbial diversity found in the acid saline lakes of Australia, Abstracts, American Society for Microbiology 106th General Meeting, Orlando, FL, N-089, pp. 388.

Hou, Y.J., Wang, J. H. and Zhu, J. L. , 2010. RESEARCH ON WATER SUPPLYING RESOURCES OF BIG AND SMALL SUGAN LAKE IN SUGAN LAKE BASIN BY USING HYDROGEN AND OXYGEN ISOTOPE. Gansu Geology(3).

Howard, A.D., Kochel, R.C. and Holt, H.E., 1987. Sapping features of the Colorado Plateau: A comparative planetary geology field guide.

Howard, A.D., Moore, J.M. and Irwin, R.P., 2005. An intense terminal epoch of widespread fluvial activity on early Mars: 1. Valley network incision and associated deposits. Journal of Geophysical Research, 110(E12): E12S14.

Hu, D., 1990. Geomorphology of Qarhan Salt Lakes. Journal of Lake Sciences(01): 37-43.

Huang, H., Huang, Q. and Ma, Y., 1996. Geology of Qaidam Basin and its petroleum prediction. Beijing: Geological Publishing House.

Huang, J. and Xiao, L., 2014. Knobby terrain on ancient volcanoes as an indication of dominant early explosive volcanism on Mars. Geophysical Research Letters: n/a-n/a.

Huang, Q., Teh-Lung, K. and Phillips, F.M., 1993. Evolutionary characteristics of lakes and palaeoclimatic undulation in the Qaidam Basin, China. Chinese Journal of Oceanology and Limnology, 11: 34-45.

Irwin, R.P., Howard, A.D. and Craddock, R.A., 2008. Fluvial valley networks on Mars, River confluences, tributaries and the fluvial network, pp. 419-451.

Jaumann, R. et al., 2007. The high-resolution stereo camera (HRSC) experiment on Mars Express: Instrument aspects and experiment conduct from interplanetary cruise through the nominal mission. Planetary and Space Science, 55(7-8): 928-952.

Jiang, H. et al., 2007. Microbial response to salinity change in Lake Chaka, a hypersaline lake on Tibetan plateau. Environmental microbiology, 9(10): 2603-2621.

Johnsson, A., Reiss, D., Hauber, E., Hiesinger, H. and Zanetti, M., 2014. Evidence for very recent melt-water and debris flow activity in gullies in a young mid-latitude crater on Mars. Icarus, 235: 37-54.

Kapp, P. et al., 2011. Wind erosion in the Qaidam basin, central Asia: Implications for tectonics, paleoclimate, and the source of the Loess Plateau. GsA Today, 21(4/5): 4-10.

Komatsu, G. and Baker, V.R., 2007. Formation of valleys and cataclysmic flood channels on Earth and

Mars. The Geology of Mars: Evidence from Earth-Based Analog, 1: 297.

Komatsu, G. et al., 2014. Drainage systems of Lonar Crater, India: Contributions to Lonar Lake hydrology and crater degradation. Planetary and Space Science, 95: 45-55.

Komatsu, G. and Ori, G.G., 2000. Exobiological implications of potential sedimentary deposits on Mars. Planetary and Space Science, 48(11): 1043-1052.

Komatsu, G., Ori, G.G., Marinangeli, L. and Moersch, J.E., 2007. Playa environments on Earth: possible analogs for Mars, The Geology of Mars: Evidence from Earth-Based Analog, pp. 322.

Kong, F., Kong, W., Hu, B. and Zheng, M., 2013a. Meterological Data, Surface Temperature and Moisture Conditions at the Dalantan Mars Analogous Site, in Qinghaitibet Plateau, China, Lunar and Planetary Science Conference, pp. 1743.

Kong, F. and Ma, N., 2010. Isolation and Identification of Halophiles from Evaporates in Dalangtan Salt Lake. Acta Geologica Sinica, 84(11): 1661-1667.

Kong, W., Zheng, M., Kong, F. and Chen, W., 2014. Sulfate-bearing deposits at Dalangtan Playa and their implication for the formation and preservation of martian salts. American Mineralogist, 99(2-3): 283-290.

Kong, W. et al., 2013b. Sedimentary salts at Dalangtan Playa and its implication for the formation and preservation of martian salts, Lunar and Planetary Science Conference, pp. 1336.

Lachenbruch, A.H., 1962. Mechanics of thermal contraction cracks and ice-wedge polygons in permafrost. Geological Society of America Special Papers, 70: 1-66.

Levy, J., Head, J. and Marchant, D., 2009. Thermal contraction crack polygons on Mars: Classification, distribution, and climate implications from HiRISE observations. Journal of Geophysical Research: Planets (1991–2012), 114(E1).

Li, J., Dong, Z., Li, E., Bao, F. and Yang, N., 2012. Grain-size Characteristics of the Deposits from Yardang Landforms in the Charhan Salt Lake Area. Journal of Desert Research(05): 1187-1192.

Li, J., Dong, Z., Li, E. and Yang, N., 2013. Wind Regime of Yardang Landform Regions in the Qarhan Salt Lake. Journal of Desert Research (05): 1293-1298.

Li, J. et al., 2016. Yardangs in the Qaidam Basin, northwestern China: Distribution and morphology. Aeolian Research, 20: 89-99.

Liu, H., Chai, H., Cheng, W., Zhong, D. and Zhou, C., 2008. A research of aeolian landform in northern China based on remote sensing imagery. Geographical Research

Lowenstein, T.K. and Hardie, L.A., 1985. Criteria for the recognition of salt‐pan evaporites. Sedimentology, 32(5): 627-644.

Lucchitta, B., 1983. Permafrost on Mars: Polygonally fractured ground, Permafrost: 4th International Conference Proceedings, pp. 744-749.

Lynch, K.L. et al., 2015. Near-infrared spectroscopy of lacustrine sediments in the Great Salt Lake Desert: An analog study for Martian paleolake basins. Journal of Geophysical Research: Planets, 120(3): 599-623.

Ma, L., Li, B. and Jiang, P., 2011. Sedimentary Features, Origin and Paleoenvironmental Significance of "Great Ear" Salt Pans in the Lop Nor Playa. Acta Sedimentologica Sinica, 29(1): 47212.

Malin, M.C. et al., 2007. Context Camera Investigation on board the Mars Reconnaissance Orbiter. Journal of Geophysical Research, 112(E5).

Malin, M.C. and Edgett, K.S., 2000. Evidence for recent groundwater seepage and surface runoff on

Mars. Science, 288(5475): 2330-2335.

Malin, M.C. and Edgett, K.S., 2001. Mars Global Surveyor Mars Orbiter Camera: Interplanetary cruise through primary mission. Journal of Geophysical Research: Planets, 106(E10): 23429-23570.

Malin, M.C. and Edgett, K.S., 2003. Evidence for persistent flow and aqueous sedimentation on early Mars. Science, 302(5652): 1931-1934.

Man, B. et al., 2015. Phylogenetic diversity of culturable fungi in the Heshang Cave, central China. Frontiers in microbiology, 6.

Mangold, N., 2005. High latitude patterned grounds on Mars: Classification, distribution and climatic control. Icarus, 174(2): 336-359.

Marchant, D.R. and Head, J.W., 2007. Antarctic dry valleys: Microclimate zonation, variable geomorphic processes, and implications for assessing climate change on Mars. Icarus, 192(1): 187-222.

Marlow, J.J., Martins, Z. and Sephton, M.A., 2011. Organic host analogues and the search for life on Mars. International Journal of Astrobiology, 10(01): 31-44.

Martín-Torres, F.J. et al., 2015. Transient liquid water and water activity at Gale crater on Mars. Nature Geoscience.

Mayer, D., Arvidson, R., Wang, A., Sobron, P. and Zheng, M., 2009. Mapping minerals at a potential Mars analog site on the Tibetan Plateau, Lunar and Planetary Science Conference, pp. 1877.

McEwen, A.S. et al., 2007. Mars Reconnaissance Orbiter's High Resolution Imaging Science Experiment (HiRISE). Journal of Geophysical Research, 112(E5).

McGill, G.E. and Hills, L.S., 1992. Origin of giant Martian polygons. Journal of Geophysical Research: Planets (1991–2012), 97(E2): 2633-2647.

Michalski, J.R. and Niles, P.B., 2010. Deep crustal carbonate rocks exposed by meteor impact on Mars. Nature Geoscience, 3(11): 751-755.

Milly, W., Yijie, W., Chenglin, L. and Yongzhi, C., 1993. The Features and Genesis of The Dalangtan Salt Deposit in the Qaidam Basin Acta Geosicientia Sinica, 1: 007.

Moore, J.M. and Howard, A.D., 2005. Large alluvial fans on Mars. Journal of Geophysical Research: Planets (1991–2012), 110(E4): 225-243.

Morris, R.V. et al., 2010. Identification of carbonate-rich outcrops on Mars by the Spirit rover. Science, 329(5990): 421-424.

Murchie, S. et al., 2007. Compact reconnaissance Imaging Spectrometer for Mars (CRISM) on Mars Reconnaissance Orbiter (MRO). Journal of Geophysical Research-Planets, 112(E5).

Musselwhite, D.S., Swindle, T.D. and Lunine, J.I., 2001. Liquid CO2 breakout and the formation of recent small gullies on Mars. Geophysical Research Letters, 28(7): 1283-1285.

Mutch, T.A., Arvidson, R.E., Head III, J., Jones, K.L. and Saunders, R.S., 1976. The geology of Mars. Princeton, NJ, Princeton University Press, 1976. 409 p., 1.

Ori, G.G., Marinangeli, L. and Komatsu, G., 2000. Martian paleolacustrine environments and their geological constrains on drilling operations for exobiological research. Planetary and Space Science, 48(11): 1027-1034.

Osinski, G., 2007. The geology of Mars: Evidence from Earth‐based analogs, edited by MG Chapman. Meteoritics & Planetary Science, 42(10): 1855-1856.

Osterloo, M. et al., 2008. Chloride-bearing materials in the southern highlands of Mars. Science,

319(5870): 1651-1654.

Osterloo, M.M., Anderson, F.S., Hamilton, V.E. and Hynek, B.M., 2010. Geologic context of proposed chloride‐bearing materials on Mars. Journal of Geophysical Research: Planets (1991–2012), 115(E10).

Paillou, P. and Rosenqvist, A., 2003. A JERS-1 radar mosaic for subsurface geology mapping in East Sahara, Geoscience and Remote Sensing Symposium, 2003. IGARSS'03. Proceedings. 2003 IEEE International. IEEE, pp. 1870-1872.

Panning, M.P. et al., 2015. Verifying single-station seismic approaches using Earth-based data: Preparation for data return from the InSight mission to Mars. Icarus, 248: 230-242.

Parker, T.J., Saunders, R.S. and Schneeberger, D.M., 1989. Transitional morphology in west Deuteronilus Mensae, Mars: Implications for modification of the lowland/upland boundary. Icarus, 82(1): 111-145.

Pechmann, J.C., 1980. The origin of polygonal troughs on the northern plains of Mars. Icarus, 42(2): 185-210.

Poesen, J., Vandaele, K. and Van Wesemael, B., 1996. Contribution of gully erosion to sediment production on cultivated lands and rangelands. IAHS Publications-Series of Proceedings and Reports-Intern Assoc Hydrological Sciences, 236: 251-266.

Pollard, W. et al., 2009. Overview of analogue science activities at the McGill Arctic Research Station, Axel Heiberg Island, Canadian High Arctic. Planetary and Space Science, 57(5): 646-659.

Qian, Z. and Liu, S., 1994. Research on aeolian and characteristics and depositional structure of lingar dunes. Journal of Desert Research.

QIN, Y.-p. et al., 2012. Magnetostrati-graphy of Liang-ZK02 Borehole in Dalangtan, Qaidam Basin and Its Paleoenvironmental Significance. Geological Re-view, 58(3): 553-564.

Rieser, A.B., Neubauer, F., Liu, Y. and Ge, X., 2005. Sandstone provenance of north-western sectors of the intracontinental Cenozoic Qaidam Basin, western China: tectonic vs. climatic control. Sedimentary Geology, 177(1): 1-18.

Rohrmann, A., Heermance, R., Kapp, P. and Cai, F., 2013. Wind as the primary driver of erosion in the Qaidam Basin, China. Earth and Planetary Science Letters, 374: 1-10.

Romig, B. et al., 2007. Desert research and technology studies 2006 report. 0148-7191, SAE Technical Paper.

Sarrazin, P. et al., 2005. Field deployment of a portable X-ray diffraction/X-ray flourescence instrument on Mars analog terrain. Powder Diffraction, 20(02): 128-133.

Schubel, K.A. and Lowenstein, T.K., 1997. Criteria for the recognition of shallow-perennial-saline-lake halites based on recent sediments from the Qaidam Basin, western China. Journal of Sedimentary Research, 67(1).

Seewald, J.S., 2001. Aqueous geochemistry of low molecular weight hydrocarbons at elevated temperatures and pressures: constraints from mineral buffered laboratory experiments. Geochimica et Cosmochimica Acta, 65(10): 1641-1664.

Sefton-Nash, E., Teanby, N.A., Newman, C., Clancy, R.A. and Richardson, M.I., 2014. Constraints on Mars' recent equatorial wind regimes from layered deposits and comparison with general circulation model results. Icarus, 230: 81-95.

Seibert, N.M. and Kargel, J.S., 2001. Small-scale Martian polygonal terrain: Implications for liquid

surface water. Geophysical Research Letters, 28(5): 899-902.

Shen, Z., 1993. The division and sedimentary environment of quaternary salt bearing strata in Qaidam basin. Geological Publishing House.

SpaceStudiesBoards, 2012. Vision and Voyages for Planetary Science in the Decade 2013-2022. National Academies Press.

Stivaletta, N., Barbieri, R., Cevenini, F. and Lopez-Garcia, P., 2011. Physicochemical conditions and microbial diversity associated with the evaporite deposits in the Laguna de la Piedra (Salar de Atacama, Chile). Geomicrobiology Journal, 28(1): 83-95.

T Neal, J., Langer, A.M. and Kerr, P.F., 1968. Giant desiccation polygons of Great Basin playas. Geological Society of America Bulletin, 79(1): 69-90.

Tamura, K. et al., 2011. MEGA5: molecular evolutionary genetics analysis using maximum likelihood, evolutionary distance, and maximum parsimony methods. Molecular biology and evolution, 28(10): 2731-2739.

Tchakerian, V.P., 1995. Desert aeolian processes. Kluwer Academic Pub.

Tonkin, T.N., Midgley, N.G., Graham, D.J. and Labadz, J.C., 2014. The potential of small unmanned aircraft systems and structure-from-motion for topographic surveys: A test of emerging integrated approaches at Cwm Idwal, North Wales. Geomorphology, 226: 35-43.

Tsoar, H., 1984. The formation of seif dunes from barchans—a discussion. Z. Geomorphol, 28(1): 99-103.

Wang, A. and Zheng, M., 2009. Evaporative Salts from Saline Lakes on Tibetan Plateau: An Analog for Salts on Mars, Lunar and Planetary Science Conference, pp. 1858.

Wang, H. et al., 2013a. Assessing the ratio of archaeol to caldarchaeol as a salinity proxy in highland lakes on the northeastern Qinghai–Tibetan Plateau. Organic Geochemistry, 54(0): 69-77.

Wang, J., Fang, X., Appel, E. and Song, C., 2012. Pliocene–Pleistocene Climate Change At the NE Tibetan Plateau Deduced From Lithofacies Variation In the Drill Core SG-1, Western Qaidam Basin, China. Journal of Sedimentary Research, 82(12): 933-952.

Wang, J., Fang, X., Appel, E. and Zhang, W., 2013b. Magnetostratigraphic and radiometric constraints on salt formation in the Qaidam Basin, NE Tibetan Plateau. Quaternary Science Reviews, 78: 53-64.

Wang, S.M., Dou, H.S., Chen, K.Z., Wang, X.C. and Jiang, J.H., 1998. Lakes in China. Sience Press.

Ward, A.W., Doyle, K.B., Helm, P.J., Weisman, M.K. and Witbeck, N.E., 1985. Global map of eolian features on Mars. Journal of Geophysical Research, 90(B2): 2038.

Warren-Rhodes, K. et al., 2007a. Searching for microbial life remotely: Satellite - to - rover habitat mapping in the Atacama Desert, Chile. Journal of Geophysical Research: Biogeosciences, 112(G4).

Warren-Rhodes, K. et al., 2007b. Robotic ecological mapping: Habitats and the search for life in the Atacama Desert. Journal of Geophysical Research: Biogeosciences, 112(G4).

Wei, X., Jiang, J. and Wang, M., 1992. Sedimentary Characteristics of Quaternary and Evolution of Saline Lake of Mahai Potash Deposit. Qinghai Geology, 1: 006.

Wu, L. et al., 2012a. EW-trending uplifts along the southern side of the central segment of the Altyn Tagh Fault, NW China: Insight into the rising mechanism of the Altyn Mountain during the Cenozoic. Science China Earth Sciences, 55(6): 926-939.

Wu, L. et al., 2012b. Two‐stage evolution of the Altyn Tagh Fault during the Cenozoic: new insight from provenance analysis of a geological section in NW Qaidam Basin, NW China. Terra Nova, 24(5): 387-395.

Wu, Q.L., Zwart, G., Schauer, M., Kamst-van Agterveld, M.P. and Hahn, M.W., 2006. Bacterioplankton community composition along a salinity gradient of sixteen high-mountain lakes located on the Tibetan Plateau, China. Applied and Environmental Microbiology, 72(8): 5478-5485.

Wu, Z., Yang, Y., Barosh, P.J., Wu, Z. and Zhang, Y., 2014. Tectonics and topography of the Tibetan Plateau in Early Miocene. Acta Geologica Sinica (English Edition), 88(2): 410-424.

Xiao, L. et al., 2012. Ancient volcanism and its implication for thermal evolution of Mars. Earth and Planetary Science Letters, 323-324: 9-18.

Xiao, L. and Wang, C., 2009. Geologic features of Wudalianchi volcanic field, northeastern China: Implications for Martian volcanology. Planetary and Space Science, 57(5-6): 685-698.

Xiao, L. et al., 2015. A young multilayered terrane of the northern Mare Imbrium revealed by Chang'E-3 mission. Science, 347(6227): 1226-1229.

Xin, Y., 1995. Windblown sand in the salt lakes in Qaidam Basin. Journal of Desert Research.

Yang, H., Pancost, R.D., Jia, C. and Xie, S., 2015. The Response of Archaeal Tetraether Membrane Lipids in Surface Soils to Temperature: A Potential Paleothermometer in Paleosols. Geomicrobiology Journal: 1-12.

Yin, A. et al., 2008a. Cenozoic tectonic evolution of Qaidam basin and its surrounding regions (Part 1): The southern Qilian Shan-Nan Shan thrust belt and northern Qaidam basin. Geological Society of America Bulletin, 120(7-8): 813-846.

Yin, A., Dang, Y.-Q., Zhang, M., Chen, X.-H. and McRivette, M.W., 2008b. Cenozoic tectonic evolution of the Qaidam basin and its surrounding regions (Part 3): Structural geology, sedimentation, and regional tectonic reconstruction. Geological Society of America Bulletin, 120(7-8): 847-876.

Yu, L., Dong, Z., Lai, Z., Qian, G. and Pan, T., 2015. Origin and lateral migration of linear dunes in the Qaidam Basin of NW China revealed by dune sediments, internal structures, and optically stimulated luminescence ages, with implications for linear dunes on Titan: Comment and Discussion. Geological Society of America Bulletin, 127(1-2): 316-320.

Yu, S.S., 1984. The Hydrochemical Feature of Salt Lakes in The Qaidam Basin. Oceanologia et Limnologia Sinica, 4: 341-359.

Yun, Y. et al., 2016. Five-Year Monitoring of Bacterial Communities in Dripping Water from the Heshang Cave in Central China: Implication for Paleoclimate Reconstruction and Ecological Functions. Geomicrobiology Journal: 1-11.

Zeng, Y., Feng, Z. and Cao, G., 2003. Desert Formation and Evolution in Qaidam Basin since the Last Glacial Epoch. Acta Geographica Sinica (03): 452-457.

Zhang, J. and Liu, E., 1985. Hydrological characteristics of streams in Qaidam Basin. Acta Geograph. Sin, 40: 242-255.

Zhang, W. et al., 2013. Late Neogene magnetostratigraphy in the western Qaidam Basin (NE Tibetan Plateau) and its constraints on active tectonic uplift and progressive evolution of growth strata. Tectonophysics, 599: 107-116.

Zheng, M., 1997. Classification of Saline Lakes and Types of Mineral Deposit, An Introduction to

Saline Lakes on the Qinghai—Tibet Plateau. Springer, pp. 79-84.

Zheng, M., Kong, W., Zhang, X., Chen, W. and Kong, F., 2013. A comparative analysis of evaporate sediments on Earth and Mars: implications for the climate change on Mars. Acta Geologica Sinica (English Edition), 87(3): 885-897.

Zheng, M. and Liu, X., 2009. Hydrochemistry of Salt Lakes of the Qinghai-Tibet Plateau, China. Aquatic Geochemistry, 15(1-2): 293-320.

Zheng, M., Tang, J., Liu, J. and Zhang, F., 1993. Chinese saline lakes, Saline Lakes V. Springer, pp. 23-36.

Zheng, M., Wang, A., Kong, F. and Ma, N., 2009. Saline lakes on Qinghai-Tibet Plateau and salts on Mars, 40th lunar planetary science conference.

Zheng, X., Zhang, M., Xu, C. and Li, B., 2002a. Salt lakes of China. China. Sci. Press: Beijing.

Zheng, X.Y., Zhang, M.G., Li, B.X. and Xu, C., 2002b. Salt Lakes of China. Science Press.

Zhou, J., Xu, F., Wang, T., Cao, A. and Yin, C., 2006. Cenozoic deformation history of the Qaidam Basin, NW China: Results from cross-section restoration and implications for Qinghai–Tibet Plateau tectonics. Earth and Planetary Science Letters, 243(1): 195-210.

Zhu, Z., 1980. An introduction of deserts in china China. Sci. Press: Beijing.